Chapter 3

Harmonic Stability with Wind Power

3.1 Introduction

In the recent years, several problems of Wind Generator tripping due to over-voltage is observed. When the problems were investigated, it is found that the harmonic current, generated by the wind generator converter, produces high voltage due to harmonic resonance. Also, several incidences have been reported of converter tripping due to over-voltage caused by the harmonics. This is the prime reason of carrying out this work to know the exact problem and to find the applicable solution. In the event of harmonic resonance, the harmonic impedance becomes very high at harmonics, whose frequency is near to resonance point and theoretically become infinite at the resonance frequency. Under the resonance condition, even a small amount of harmonic current is enough to produce high harmonic voltage drop, which is ultimately resulting in overall voltage distortion. There are various methods to analyse the harmonic problem. Generally, the frequency scan method has been used to locate the harmonic resonance point. Though, it is simple and easy to use, but it does not give information about the participation of different network components and also how the resonant point is affected by changes in the value of the components. To analyse the problem, several techniques were investigated. Finally, based on the ease of use and potential of in-depth analysis, the Modal analysis has been adopted for analyzing the problem in this work. In conventional power generation, harmonics are virtually not generated by the generators. Also, the resonance condition does not prevail on the generator bus because of absence of shunt capacitors. But, both of these are present in the Wind Farm. It may impact significantly, if the

resonance point coincides with the one of the frequencies of generated harmonic currents. Harmonic Resonance can become complicated, because of complex network configuration and presence of multiple harmonic sources in the network. A power system network contains many inductive, capacitive and resistive elements. An interaction among inductive and capacitive elements leads to oscillations. The period of oscillation depends on the resistive component. Though, the resistive elements cause the loss of power, but they also act as a damping element, which reduces the harmonic magnitude exponentially and supports the harmonic stability. The exchange of energy between capacitive and inductive elements appears as an oscillations, the frequency of oscillation depends on the value of participating capacitor and inductor value. Such a network is characterized by the critical frequency, known as resonance frequency. If such a network is excited by the source having resonance frequency, it will lead to a sustained oscillation. Traditionally, the frequency scan analysis is a primary tool to find out the resonance in the system, but this technique does not give following informations.

1. Which combinations of L & C are involved in the resonance?
2. How many modes are participating in a given resonance?
3. What is the sensitivity of a resonance w.r.t different network element/component?
4. The effect of resonance on different buses of the network?
5. Which is the most effective way to avoid the harmonic resonance?

To answer these questions, a survey has been made and suitable analysis method has been selected, which has been presented in this work.

All wind parks are unique in characteristics. They all have resonance frequencies that are dependent on various factors like grid topology, connected generators, and reactive power equipment used. Furthermore, the impedance and the resonance points of Wind Park changes with the change in number of turbine and capacitor or filter banks in operation. The connecting cable has also a predominant effect on the resonance frequency. The internal cable connections in a Wind Park connect each turbine of the wind park to the wind park transformer, whereas the transmission cable connects the wind park transformer to the nearby substation [319]. The total length of the cable varies from a few kilometers to few tens of kilometers. The length of cable, and hence the cable

capacitance plays an important role in harmonic resonance. Presence of capacitor banks and shunt/series reactors also increase the possibility of resonance in the wind power plant. Several capacitors are connected in the form of bank to improve the power factor and reduce the reactive power absorption from grid [320]. The capacitor bank at the PCC level is also used to support the voltage in abnormal conditions. There may be shunt reactors connected to cable to compensate high capacitance of a cable. All these components create conducive conditions for harmonic resonance.

In this work, a systematic approach has been presented. Starting with the admittance matrix formation, followed by the finding of eigenvalues for discrete frequency points. At resonance or critical frequency, eigenvalue becomes very low or zero. These eigenvalues are then analysed further to find out the effect of change in a network element on this eigenvalues. The network configuration keeps on changing, depends on the operational requirement, so the eigenvalue and critical frequency also keeps on changing. This is the reason, why it becomes imperative to find out, how firm or steady is any resonance point?

In this chapter, the harmonic stability of network has been assessed and the solution to improve performance is also suggested.

3.2 Harmonics Resonance

Harmonic resonance is an extraordinarily diverse and varied phenomenon seen in countless forms throughout the universe, from gravitational orbital resonances, to electromagnetic oscillations, to acoustical vibrations in solids, liquids, and gases, to laser resonance in light and microwaves. Harmonic Resonance observed in power system is Electromagnetic. It is basically a interaction of energy between capacitive and inductive elements. Since, there are numerous capacitive and inductive elements in power system, the harmonics resonance phenomena becomes complicated. In a simple circuit having one capacitor and one inductor, it is easy to find out the resonance frequency, given by equation.

$$f_h = \frac{1}{\sqrt{LC}} \tag{3.1}$$

But with increase in number of such elements, it becomes difficult to calculate the resonance frequency by conventional way of calculation. This is probably one of the reason for requirement of an inclusive method which can give complete insight of problem. Any

tool which unveil the complex relationship between energy storing elements, can help to understand the phenomena of resonance. This can also be useful to mitigate harmonic resonance effectively. As there are number of storing elements, there will be number of oscillating interactions in the system. Every harmonic resonance is unique in nature and its origin can be attributed to a group of storing elements. Thus, it is important to know which components are involved in a given harmonic oscillation. Different Harmonic oscillations can be observed from different buses and all these harmonics oscillations are not originating from the same source. The source decides how long harmonic oscillation propagate in the system.

There are various methods proposed in literatures to analyse the harmonic resonance phenomena. This methods are enlisted here.

- **State Space Method**: The State Space Method is based on the eigenvalue analysis of the network. The state space matrix is formulated using the differential equations of inductor current and capacitor voltage. This technique was originally proposed to study and anlyse the transient characteristics of a network. The state space technique is applied to linear system. But, it can also be applied to non-linear system after linearizing of equation. This method is very widely been applied for small signal stability analysis. The same can be applied for power system network analysis. The difference lies in the selection of state variable. In harmonic resonance analysis, the voltages of capacitors and currents of inductors are taken as state variables. Reference [321] can be referred for detail about this method.

- **Newton Raphson Method**: This method is influenced by the popular load flow method based on Newton - Raphson algorithm. It was proposed in [320] to shift the poles and zeros of transfer function to specify locations in complex plane. The objective of shift is to reduce harmonic voltage. This method is based on the fact that, the poles and zeros are sensitive to the change in system parameters. The calculations are done in s-domain using Admittance Matrix $Y(s)$. First, the network is modelled in form of admittance matrix $Y(s)$. The admittance matrix is same as the nodal admittance matrix of power system. The diagonal element y_{ii} is calculated by summing all admittances connected to node$-i$. The admittance matrix is differentiated with respect to complex frequency s. This method is discussed in

reference [319] in detail.

- **Descriptor Method**: This method is proposed by Varricchio [322] to improve the harmonic performance. The difference between this method and other method is the modelling approach. In descriptor technique, all inductive currents and all capacitive voltages are considered as a state variables. In this method care has to be taken regarding the redundancies of state variable. However, there are no restrictions on minimum number of state variable. Three sets of equations; differential, algebraic and KCL equation at each node represent the complete descriptor system. The KCL equation defines the electrical connections among the several circuit elements. So, it represents the network topology. This method has potential to analyse the circuit in deep, but it is complicated as far as the application to large network is concerned. For large and sparse network, labour involved is unjustifiable. So, the application of descriptor method remain limited to the small and medium scale industrial system only.

- **Modal Analysis**: This method is based on the eigenvalues of the admittance matrix. There are several variants of this method found in literatures [323], [324], [325]. This method is quite simple and easy to apply. It is found in several literature, but it's application is limited to find the resonance and sensitivity only [326]. However, the utility of sensitivity of resonance is not further explored. In this work, Modal analysis is taken further and used to find the contribution by different network element to harmonic resonance. In this work, the utility of this method is explored and applied to improvise the harmonic voltage. The Modal analysis is discussed in detail in next section.

3.3 Modal Analysis

Modal analysis is the study of the dynamic properties of systems in the frequency domain. It has been widely used in various domains like stress and vibration analysis, noise pattern analysis, electrodynamics etc. The most common type of analysis is quasi-static analysis, where the input is applied at a very slow rate, so that, the rate of change of input is negligible (or almost zero). Dynamic analysis is important, as the effects of rate of change of input cannot be ignored. Both types provide one-to-one relationship between

particular inputs (for example, an input applied to system) to its system response (for example, deterioration of the voltage due to Harmonic current).

In contrast to quasi-static and dynamic, Modal analysis provides an overview of the limits of the response of a system. For example, for a particular input (like supply of harmonic current of certain amplitude and frequency), what will be the limits of systems response (for example, what will be the maximum harmonic voltage).

Every object has an internal frequency (or resonant frequency) at which the object can vibrate naturally. It is also the frequency, where the object will allow a transfer of energy from one form to another with minimal loss. In electrical system, it is from electromagnetic to electrostatic. As the frequency increases towards the resonant frequency, the amplitude of response asymptotically increases to infinity. In other words, the result of Modal analysis are critical frequencies at which the amplitude increases to infinity.

Modal analysis technique is also known as eigen-analysis technique, eigenvalue or eigenmode analysis. This technique is not limited to systems with linear differential equations. But, it is applicable to all systems involving matrices. It is essentially a matrix decoupling technique. In power system domain, eigenvalue analysis has been initially applied to the problem of dynamic stability. It has also been applied for symmetrical component analysis. Now, It has been used widely in power system to address various problems like voltage stability, small signal stability or dynamic stability and harmonic stability.

In this work, Modal analysis application for harmonic analysis or resonance analysis has been explained in detail. The relation of harmonics voltage due to harmonic current is given by equation (3.2)

$$[V_h] = [Y_h]^{-1}[I_h] \tag{3.2}$$

Where, $[Y_h]$ is the network admittance matrix at harmonic frequency of order h. $[V_h]$ is the nodal voltage and $[I_h]$ the nodal current injection respectively. At resonance frequency, impedance increases sharply. This amplifies the harmonic current and exhibit as harmonic voltage. It is worth noting that even small harmonic current can produce high harmonic voltage due to high harmonic impedance. As the frequency reaches near the resonant point, admittance matrix $[Y_h]$ approaches singularity. How admittance matrix

$[Y_h]$ attains singularity is an interesting way to understand the harmonic resonance problem. The essence of this problem is harmonic resonance. Using eigenanalysis technique, the admittance matrix $[Y_h]$ can be decomposed in to following form:

$$[Y_h] = [L][\Lambda][R] \tag{3.3}$$

where, the diagonal matrix $[\Lambda]$ is eigenvalue matrix, $[L]$ and $[R]$ are the left eigenvector and right eigenvector respectively. Substituting, (3.3) in (3.2) and omitting suffix h for simplification.

$$[V] = ([L][\Lambda][R])^{-1}[I] \tag{3.4}$$

$$[V] = [R]^{-1}[\Lambda]^{-1}[L]^{-1}[I] \tag{3.5}$$

Since the admittance matrix is symmetrical for symmetrical network, the left and the right eigenvector is related by equation following equation.

$$[L] = [R]^{-1} \tag{3.6}$$

Using relation as per (3.6), the equation (3.5) can be given as,

$$[V] = [L][\Lambda]^{-1}[R][I] \tag{3.7}$$

Multiplying both side by right eigenvector $[R]$,

$$[R][V] = [R][L][\Lambda]^{-1}[R][I] \tag{3.8}$$

$$[R][V] = [\Lambda]^{-1}[R][I] \tag{3.9}$$

$$[U] = [\Lambda]^{-1}[J] \tag{3.10}$$

Where $[U] = [R][V]$ is Modal voltage vector and $[J] = [R][I]$ is Modal current vector. Expanding equation (3.10) in matrix form.

$$\begin{bmatrix} U_1 \\ U_2 \\ \cdots \\ U_n \end{bmatrix} = \begin{bmatrix} \lambda_1^{-1} & 0 & 0 & 0 \\ 0 & \lambda_2^{-1} & 0 & 0 \\ 0 & 0 & \cdots & 0 \\ 0 & 0 & 0 & \lambda_n^{-1} \end{bmatrix} \begin{bmatrix} J_1 \\ J_2 \\ \cdots \\ J_n \end{bmatrix} \tag{3.11}$$

Where λ is Modal admittance (Y_m) and λ^{-1} is Modal impedance (Z_m). For small value of λ_1, the current injection J_1 will produce large Modal voltage U_1. It is important to note that due to decoupling, other Modal voltages are not affected due to Modal current J_1. The resonance takes place when the system modes are matching with the harmonics order of injected current. Only injected current will not result in resonance and similarly presence of specific system modes alone cannot create harmonic resonance. The critical eigenvalue is identified by its magnitude. Smallest eigenvalue is known as a critical eigenvalue or critical mode. The eigenvectors corresponding to critical eigenvalues are known as critical left and critical right eigenvectors.

The Modal current is a abstract concept, which is represented by linear combination of actual current injection at different buses.

$$\begin{bmatrix} J_1 \\ J_2 \\ \cdots \\ J_n \end{bmatrix} = \begin{bmatrix} T_{11} & T_{12} & \cdots & T_{1n} \\ T_{21} & T_{22} & \cdots & T_{2n} \\ T_{31} & T_{32} & \cdots & T_{3n} \\ T_{n1} & T_{n2} & \cdots & T_{nn} \end{bmatrix} \begin{bmatrix} I_1 \\ I_2 \\ \cdots \\ I_n \end{bmatrix} \tag{3.12}$$

From equation (3.12), it is clear that the Modal current is a joint contribution of all nodal currents. The Modal currents and nodal currents are related by the right and left eigenvector. For example, if T_{11} is significantly large than Modal current J_1 is mainly contributed by nodal current I_1.

$$J_1 \approx T_{11} I_1 \tag{3.13}$$

The Modal currents produces Modal voltages. The Modal voltages are given by

$$U_1 \approx \lambda^{-1} J_1 \tag{3.14}$$

Using relation given in equation (3.13),

$$U_1 \approx \lambda^{-1} T_{11} I_1 \tag{3.15}$$

The Modal voltages are related to nodal voltages by,

$$\begin{bmatrix} U_1 \\ U_2 \\ \cdots \\ U_n \end{bmatrix} = \begin{bmatrix} R_{11} & R_{12} & \cdots & R_{1n} \\ R_{21} & R_{22} & \cdots & R_{2n} \\ R_{31} & R_{32} & \cdots & R_{3n} \\ R_{n1} & R_{n2} & \cdots & R_{nn} \end{bmatrix} \begin{bmatrix} V_1 \\ V_2 \\ \cdots \\ V_n \end{bmatrix} \tag{3.16}$$

The physical nodal voltages at each bus or node derived from Modal voltage using following relation.

$$\begin{bmatrix} V_1 \\ V_2 \\ \cdots \\ V_n \end{bmatrix} = \begin{bmatrix} L_{11} & L_{12} & \cdots & L_{1n} \\ L_{21} & L_{22} & \cdots & L_{2n} \\ L_{31} & L_{32} & \cdots & L_{3n} \\ L_{n1} & L_{n2} & \cdots & L_{nn} \end{bmatrix} \begin{bmatrix} U_1 \\ U_2 \\ \cdots \\ U_n \end{bmatrix} \tag{3.17}$$

$$\begin{bmatrix} V_1 \\ V_2 \\ \cdots \\ V_n \end{bmatrix} = \begin{bmatrix} L_{11} \\ L_{21} \\ \cdots \\ L_{n1} \end{bmatrix} \begin{bmatrix} U_1 \end{bmatrix} + \begin{bmatrix} L_{12} \\ L_{22} \\ \cdots \\ L_{n2} \end{bmatrix} \begin{bmatrix} U_2 \end{bmatrix} + \cdots + \begin{bmatrix} L_{1n} \\ L_{2n} \\ \cdots \\ L_{nn} \end{bmatrix} \begin{bmatrix} U_n \end{bmatrix} \tag{3.18}$$

For larger value of U_1 as compared to other Modal voltages, the nodal voltages are approximated by,

$$\begin{bmatrix} V_1 \\ V_2 \\ \cdots \\ V_n \end{bmatrix} \approx \begin{bmatrix} L_{11} \\ L_{21} \\ \cdots \\ L_{n1} \end{bmatrix} \begin{bmatrix} U_1 \end{bmatrix} \tag{3.19}$$

This reveals that the Modal voltage U_1 contributes to nodal voltages. This contribution is designated using left eigenvector $[L_{11}, L_{21}, \cdots, L_{n1}]^T$. The nodal voltages are dependent on the respective component of eigenvector. From above discussion, it can be summarised that the right eigenvector exhibits the excitability or stimulation of critical mode, whereas the left eigenvector shows the obserbability of the critical mode. The bus with the largest right eigenvector element is the bus having highest potential to excite the mode and that with the largest left eigenvector element is the one having the highest observability. The excitability is also related with the controllability. The bus with highest excitability is the most effective location to inject the counter current to cancel harmonics.

The theory for selective Modal analysis [259] is used for critial mode analysis. For simplification, controllability and excitability are combined in to single index.

$$\begin{bmatrix} V_1 \\ V_2 \\ \cdots \\ V_n \end{bmatrix} \approx \begin{bmatrix} L_{11} & L_{12} & \cdots & L_{1n} \\ L_{21} & L_{22} & \cdots & L_{2n} \\ \cdots & \cdots & \cdots & \cdots \\ L_{n1} & L_{n2} & \cdots & L_{nn} \end{bmatrix} \begin{bmatrix} \lambda_1^{-1} & 0 & 0 & 0 \\ 0 & 0 & 0 & 0 \\ 0 & 0 & \cdots & 0 \\ 0 & 0 & 0 & 0 \end{bmatrix} \begin{bmatrix} R_{11} & R_{12} & \cdots & R_{1n} \\ R_{21} & R_{22} & \cdots & R_{2n} \\ \cdots & \cdots & \cdots & \cdots \\ R_{n1} & R_{n2} & \cdots & R_{nn} \end{bmatrix} \begin{bmatrix} I \end{bmatrix} \tag{3.20}$$

$$\begin{bmatrix} V_1 \\ V_2 \\ \cdots \\ V_n \end{bmatrix} \approx \lambda_1^{-1} \begin{bmatrix} L_{11}R_{11} & L_{11}R_{12} & \cdots & L_{11}R_{1n} \\ L_{21}R_{11} & L_{21}R_{12} & \cdots & L_{21}R_{1n} \\ \cdots & \cdots & \cdots & \cdots \\ L_{n1}R_{11} & L_{n1}R_{12} & \cdots & L_{n1}R_{1n} \end{bmatrix} \begin{bmatrix} I_1 \\ I_2 \\ \cdots \\ I_3 \end{bmatrix} \tag{3.21}$$

The nodal voltages as per equation (3.21) is derived, based on the fact that the Modal impedance Z_1 $\frac{1}{\lambda_1}$, is much larger than other Modal impedances. The diagonal element of matrix in (3.21) is defined as the participation factor. Participation factor PF_{jk} is given by,

$$PF_{jk} = L_{jk}R_{kj} \tag{3.22}$$

Where j is the bus number and k is the mode number.

As already discussed, the critical mode is defined as the minimum eigenvalue. To consider as critical mode, the eigenvalue should sufficiently small. But, one obvious question

arises, how to define the sufficiency? This can be better explained with argument that the sufficient word depends on harmonic current with frequency equal to critical mode frequency. The ultimate aim is to keep nodal harmonic voltages under control. If harmonic current is very high, then even value which is not very small should be treated as critical value.

The frequency at which any eigenvalue approaches very small value (at critical mode) is known as Modal resonance frequency. Whereas the frequency at which the impedance reaches its peak value is known as harmonic resonance frequency. For any given circuit there may be multiple harmonics frequencies observed in form of multiple harmonic peaks. But, this may be related with same critical mode. The frequency scan can show multiple resonance frequencies because of combined effect of different modes. The impedance at any bus say i is given by Z_{ii}.

$$Z_{ii} = PF_{i1}\lambda_1^{-1} + PF_{i2}\lambda_2^{-1} + \cdots + PF_{in}\lambda_n^{-1} \tag{3.23}$$

$$Z_{ii} = PF_{i1}Z_{m1} + PF_{i2}Z_{m2} + \cdots + PF_{in}Z_{mn} \tag{3.24}$$

The first digit of PF subscript is bus number and second digit is mode number. The maximum value of impedance depends on the resistive elements in the circuit. By reducing the resistive elements minimum value of λ can be made very small. The domination of Modal impedance on bus impedance depends on the participation factor. For example, if PF_{i1} is high, the Modal impedance Z_{m1} dominates. This is how the resonance frequency is related with the Modal resonance frequency. The PF is sufficient enough for Modal analysis. The magnitude of participation factor signifies how far the resonance will propagate deep in to the system. The bus with highest participation factor is considered as the ***resonance center***.

For symmetrical network, the left and right eigenvectors are related as per equation (3.6). The eigenvalue and eigen vectors are defined as

$$[\Lambda] = [L]^{-1}[Y_h][L] \tag{3.25}$$

For symmetrical $[Y_h]$ matrix and diagonal $[\Lambda]$ matrix,

$$\begin{aligned}[\Lambda] &= [\Lambda]^{-1} = ([L]^{-1}[Y_h][L])^T \\ &= [L]^T[Y_h]^T([L]^{-1})^T = [L]^T[Y_h]([L]^{-1})^T\end{aligned} \tag{3.26}$$

From equation (3.25) and (3.26), we can conculde that,

$$[L]^T = [L]^{-1} = [R] \tag{3.27}$$

Some of the important observations can be made from this relation. For bus having highest excitation level for any given mode, the same bus will have highest observation level also for the same mode. This means that the harmonics current injection into this bus will amplify the harmonics voltage and it can be observed on the same bus.

3.3.0.1 Sensitivity of Eigenvalue

The right eigenvector R_i and left eigenvector L_i associated with i^{th} eigenvalue λ_i satisfy the following two relations.

$$[Y_h]R_i \quad = \lambda_i R_i \tag{3.28}$$

$$L_i^T[Y_h] \quad = L_i^T\lambda_i \tag{3.29}$$

Rearranging above equations.

$$[Y_h - \lambda_i I]R_i = 0 \tag{3.30}$$

$$L_i^T[Y_h - \lambda_i I] = 0 \tag{3.31}$$

Assuming that the eigenvalues and eigenvectors vary continuously with respect to the element of $[Y_h]$ matrix.

$$(Y_h + \Delta Y_h)(R_i + \Delta R_i) = (\lambda_i + \Delta\lambda_i)(R_i + \Delta R_i) \tag{3.32}$$

Expanding above equations,

$$[Y_h R_i] + [\Delta Y_h R_i + Y_h \Delta R_i] + [\Delta Y_h \Delta R_i] = [\lambda_i R_i] + [\Delta\lambda_i R_i + \lambda_i \Delta R_i] + [\Delta\lambda_i \Delta R_i] \tag{3.33}$$

Neglecting the second order terms $[\Delta Y_h \Delta R_i]$ and $[\Delta\lambda_i \Delta R_i]$ for small purturbation.

$$[Y_h - \lambda_i I]\Delta R_i + \Delta Y_h R_i = \Delta\lambda_i R_i \tag{3.34}$$

Multiplying equation (3.34) by $[L_i]^T$ on both side,

$$[L_i]^T[Y_h - \lambda_i I]\Delta R_i + [L_i]^T[\Delta Y_h R_i] = [L_i]^T[\Delta\lambda_i R_i] \tag{3.35}$$

The first term on the left hand side of equation (3.35) is zero.

$$[L_i]^T[\Delta Y_h R_i] = [L_i]^T[\Delta\lambda_i R_i] \tag{3.36}$$

Assuming that the k^{th} diagonal entry of $[Y_h]$ matrix is purturbed,

$$\left[\Delta Y_h\right] = \begin{bmatrix} 0 & 0 & \cdots & 0 \\ 0 & \Delta y_{kk} & \cdots & 0 \\ \vdots & \vdots & \vdots & \vdots \\ 0 & 0 & \cdots & 0 \end{bmatrix} \tag{3.37}$$

Simplifying the left hand side of equation (3.36).

$$L_i^T \Delta Y_h R_i = L_{ki}^T \Delta y_{kk} R_{ik} = L_i^T \Delta\lambda_i R_i \tag{3.38}$$

Finally, solving for sensitivity gives,

$$\frac{\Delta\lambda_i}{\Delta y_{kk}} = \frac{L_{ki} R_{ik}}{L_i^T R_i} = PF_{ki} \tag{3.39}$$

As $L_i^T R_i = 1$,

$$\frac{\Delta\lambda_i}{\Delta y_{kk}} = L_{ki} R_{ik} = PF_{ki} \tag{3.40}$$

3.3.1 Relation between Critical Mode and Resonance Frequency

The frequency scan of the network show different resonance frequency on different bus. But, they could relate to the same resonance mode. The reason behind different resonance peaks at different bus is the system resistance. The resistance between two buses separates the resonance frequency. The relationship of bus impedance to the Modal impedance is very important to understand the system behaviour to different frequencies. The modes are considered as critical, if eigenvalue is enough small to produce harmful resonance. The threshold or smallness of eigenvalue could be system dependent. The number of resonant modes is equal to the number of capacitive elements in the system. With the help of Modal analysis, we can actually find the number of resonance frequencies associated with the given critical mode. The frequency scan may show the different resonance frequencies, as the frequency scan impedances are the result of different Modal impedance with different participation factor.

In ideal condition, $[Y]$ matrix become singular at critical frequency. In actual condition, due to the presence of finite none-zero resistance in the system, at resonance, the eigenvalue becomes very low and its value depends on the resistance value. As the resistance value is reduced, the minimum value of all eigenvalues approaches zero. One more fact drawn from Modal analysis technique is the relationship between number of modes and the number of passive elements in the system. The number of modes is equal to the number of capacitive elements in the system. This is explained with an example in the section "Network Aggregation".

3.3.2 Determination of Critical Mode

Determination of system resonant frequencies using finding of critical mode is possible by finding out the eigenvalue of Y matrix at discrete frequencies. System resonant frequencies can be located from Admittance-frequency curves of the Modal Admittance, where admittance approaches vary low value, near to zero. The procedure of resonance

determination by using Modal analysis is illustrated in flow chart given in figure (3.1). The maximum magnitude of Modal impedances at a resonance can be interpreted as the degree of resonance severity. Plot impedance-frequency curve and identify the peaks from curve. Now reduce the Δi, and run the scan again between two frequency value, where the peaks are observed. Stop the scan when $i<i_{min}$

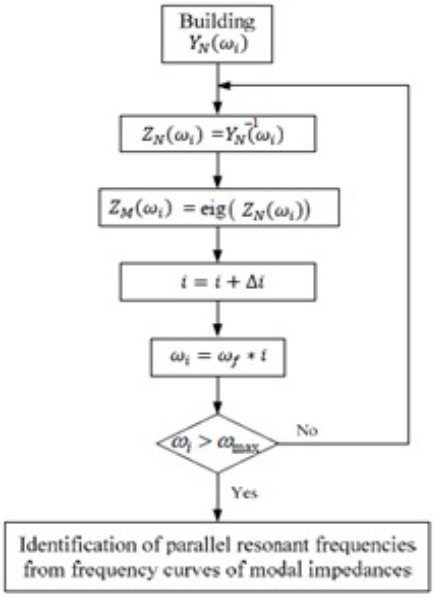

Figure 3.1: Flowchart for Critical Frequency Determination

The Modal analysis of simple circuit is carried out here. A 10 km long cable of 33 kV, 100 mm^2 is connected to the Power system. The cable capacitance is halved and lumped at the both end of the cable. The system resistance is varied from 0.04 Ω to 4 Ω. The effect of increase in resistance can be seen in the peak value of Modal impedance. The peak value of Modal impedance decreases with increase in resistance value. Figure 3.3 shows Modal Impedance of circuit shown in figure 3.2.

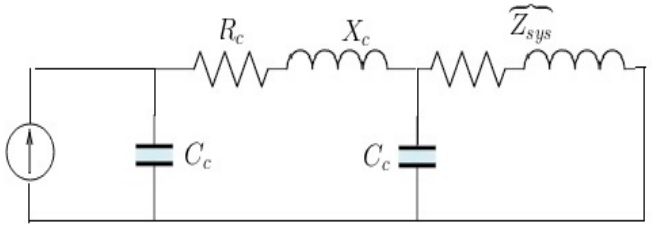

Figure 3.2: Cable Connected to System

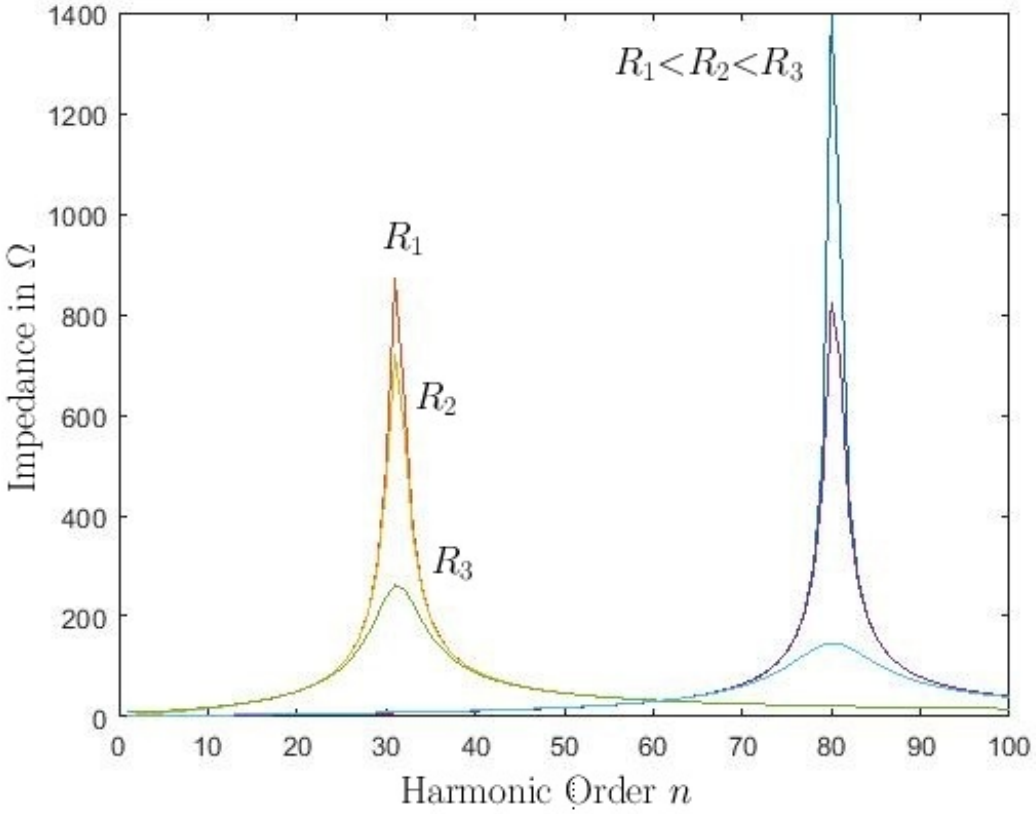

Figure 3.3: Modal Impedance of Cable Connected to Line.

Table 3.1: Network Parameter

R varies from 0.04 to 4 Ω		
Sr. No	Parameter	Value
1	R_c	2.48 Ω
2	X_c	$\jmath$1.11 Ω
3	C_c	2.2 μF
4	Z_{sys}	R+$\jmath$ 0.3 Ω

Capacitance of cable can be modelled either as 'π' model or 'T' model. The effect of modelling has been explained with example. Figure 3.3 shows the Modal analysis of 'π'

model, where two modes are observed. This is due to presence of two capacitors as shown in figure 3.2. The cable with 'T' model is shown in figure 3.4. It has only one capacitor, which represents the total capacitance of cable. The Modal analysis of 'T' circuit is shown in figure 3.5. The difference in Modal impedance due to difference in modelling of cable capacitance can be seen by comparing figures 3.3 and 3.5.

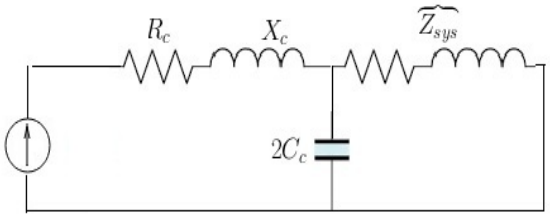

Figure 3.4: Circuit with "T" Equivalent Model of Cable

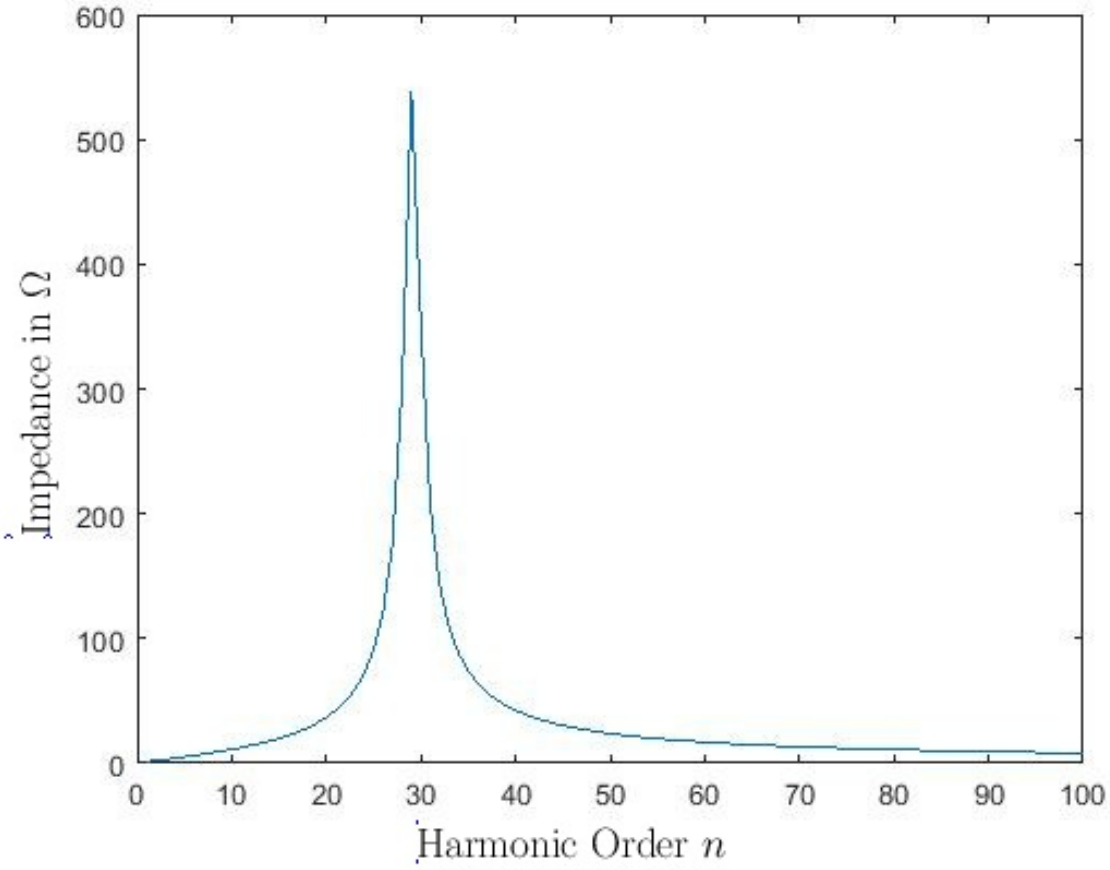

Figure 3.5: Modal Impedance of Cable represented as "T" Model.

The critical frequency obtained from Modal analysis can be easily verified by analytical method. The first mode of network shown in 3.2 is a result of capacitor C_c and parallel impedance of cable and system i.e $Z_{cable}||Z_{sys}$. It is given over here.

$$f_h = \sqrt{\frac{1428.6}{0.236}} = 77.8 \tag{3.41}$$

Whereas, the second mode is the result of capacitor C_c and total impedance of cable and system i.e $Z_{cable} + Z_{sys}$.

$$f_h = \sqrt{\frac{1428.6}{1.41}} = 31.8 \tag{3.42}$$

Similarly, for 'T' equivalent circuit, it is a result of capacitor C_c and impedance of system i.e Z_{sys}. It is given by,

$$f_h = \sqrt{\frac{714}{0.85}} = 29 \tag{3.43}$$

These results can be compared with the results of Modal analysis. It can be inferred that the analytical results are in line with the Modal analysis. This proves the utility of Modal analysis.

3.3.2.1 Network Aggregation

The number of modes are dependent on the depth of detailing of network model. Higher the detailing, more will be the number of modes appear. But detailing involves labour and increases the dimension of Y matrix. So, there is a trade of between detailing of the circuit and resolution of results. To concentrate on the network part of interest, the remaining part is generally aggregated and presented as lumped parameter contains more than one elements. Here the effect of aggregation is explained using example. The figure 3.6 shows the network and figure 3.7 shows the frequency response of network. The network parameters are same as network used in section (3.3.2).

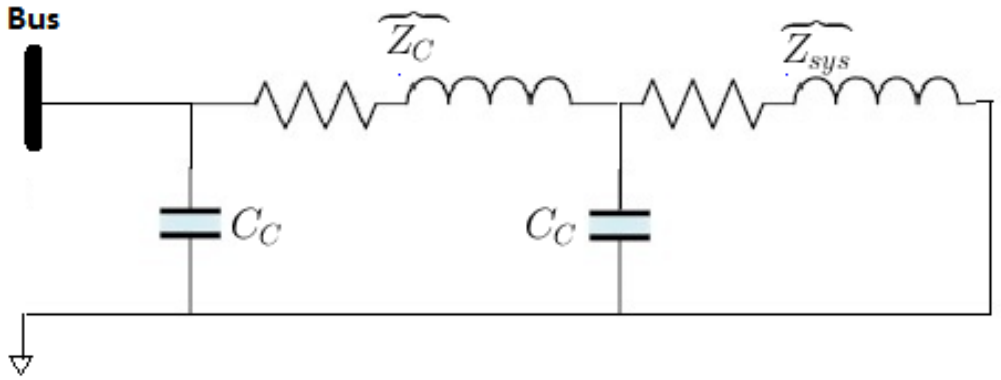

Figure 3.6: Network Aggregation

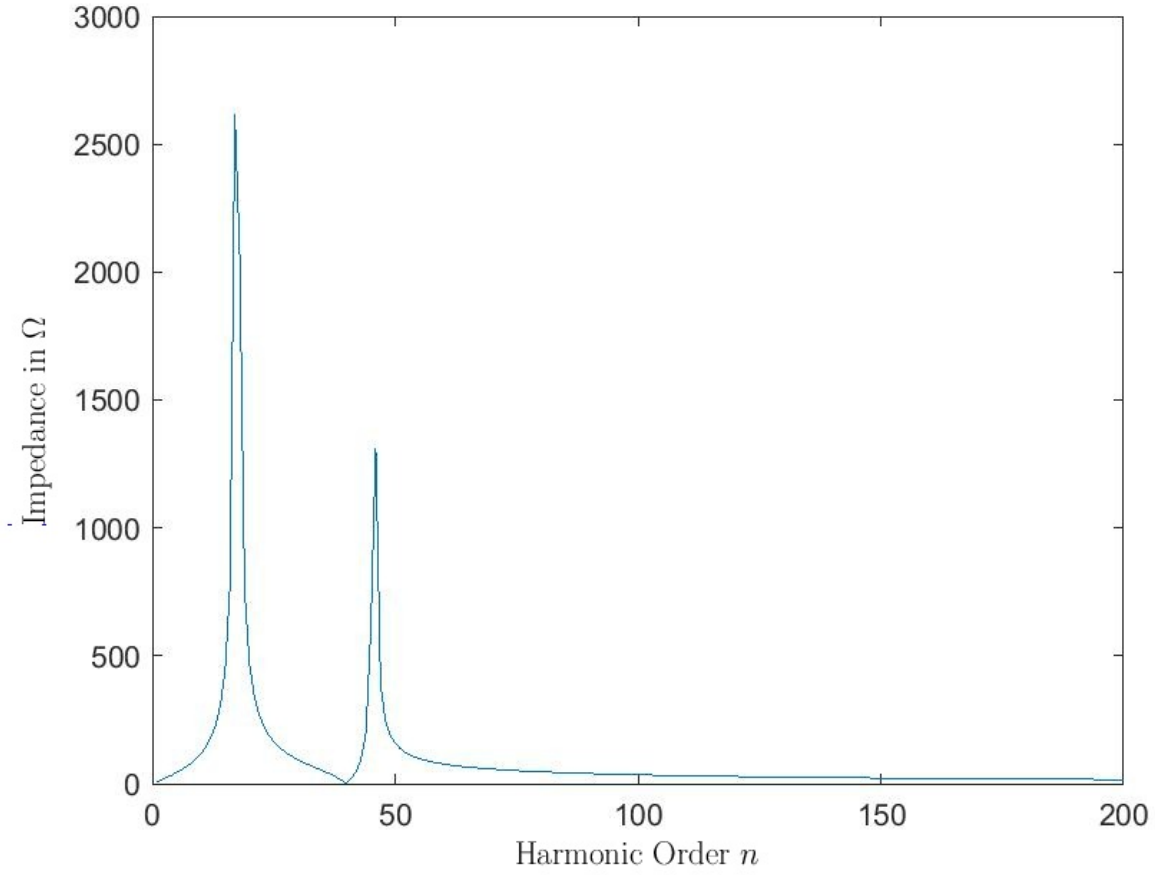

Figure 3.7: Modal Impedance of Aggregated Network

In figure 3.6 two peaks are observed in one nodal impedance. This is due the aggregation of network. The network given in figure 3.5 contains two capacitors. Each capacitor contributes one peak in the mode. The contribution of network elements to each impedance peak is difficult task with nodal analysis, but it can be very well performed with Modal analysis, if network is modelled in detail. To perform verification the analytical technique can be used. One more difficulty with aggregated network is to calculate sensitivity of component with respect to multiple components in aggregated network.

3.4 Selection of Method for Harmonic Resonance Analysis

Following points are considered for selection of method.

1. Though, State Space Method and Descriptor Method directly give the resonant points, but these are difficult to implement due to requirement of formulation of many equations.
2. Newton Raphson (NR) method is useful to relocate the poles and zeros of network, but still it is difficult when used for finding of network resonant points. Also, it requires differentiation of admittance matrix.
3. All this methods become difficult to use with complex network structure.
4. It is directly not possible to set up relationship between network parameter/component and resonant frequency or mode
5. State Space Analysis and Descriptor method doesn't give network impedance at resonant point, so it is difficult to comment on severity of resonant frequency or mode.
6. Newton Raphson method only works on the part of the network and neglect the rest of the network
7. All of the above mentioned method are difficult to use with optimization algorithm
8. Modal analysis overcomes all of the above drawbacks. This makes Modal Analysis ideal for analysis purpose.
9. It has only one drawback; it does not give resonant point directly, resonant points has to be found out by evaluating network admittance at discrete frequency points.
10. Modal Analysis establishes the relationship between different resonant modes and network components.
11. Using Modal Analysis, it is also possible to find sensitivity of resonant modes with respect to network components. This helps us in modification or change in resonance point effectively.

3.5 Optimization using Simulated Annealing

Simulated Annealing is a method of solving constrained and un-constrained optimization problems. The method models the physical process of heating a material and slowly lowering the temperature to decrease the chance of creation of fatigue and defects in the material.

At each iteration of the simulated annealing algorithm, a new point is randomly generated. The distance of the new point from the current point, or the extent of the search, is based on a probability distribution with a scale proportional to the temperature. The algorithm accepts all new points that lower the objective, but also, with a certain probability, points that raise the objective. By accepting points that raise the objective, the algorithm avoids being trapped in local minima, and is able to explore globally for more possible solutions. An annealing schedule is selected to systematically decrease the temperature as the algorithm proceeds. As the temperature decreases, the algorithm reduces the extent of its search to converge to a minimum.

Simulated Annealing (SA) is one of the meta-heuristic method of solving difficult optimization problem. It is particularly used when objective function is not clearly define in mathematical form. It is used for black box optimization problem. It is widely applied in many real life problems. It is simple in application and it is an advantage of SA. It is conceptualized from the physical heating-cooling process. It avoids the drawback of Monte-Carlo approach, which can be trapped in local minima. SA is useful where large population based algorithms are not possible. For example, complex simulation processes that manipulate a large dimension state-space. The section is organized as per following. First, the basic of SA algorithm is introduced. In the next section, the properties of SA are briefly presented. Then, practical issues in implementation of SA is discussed. Finally, problem of Modal impedance reduction is depicted.

3.5.1 Basic of Simulated Annealing

The concept of SA algorithm is first introduced by three researchers at IBM. The concept is based on a strong analogy with the physical annealing of materials. Annealing is a process, which brings solid to a low temperature after its temperature is raised. It has two main steps. Bring the solid to a very high temperature (up to melting point) Cool the solid according to a very particular temperature decreasing scheme in order to reach a

solid state of minimum energy. In a liquid state, the molecules of material are distributed very randomly. It is exhibited that, the minimum energy level is only reached, if the material is cooled down very slowly in sufficiently long time. If the material is not cooled down slowly, the solid will be in the metastable state with non-minimal energy; this is referred to as a hardening, which would be the case with sudden cooling of a solid.

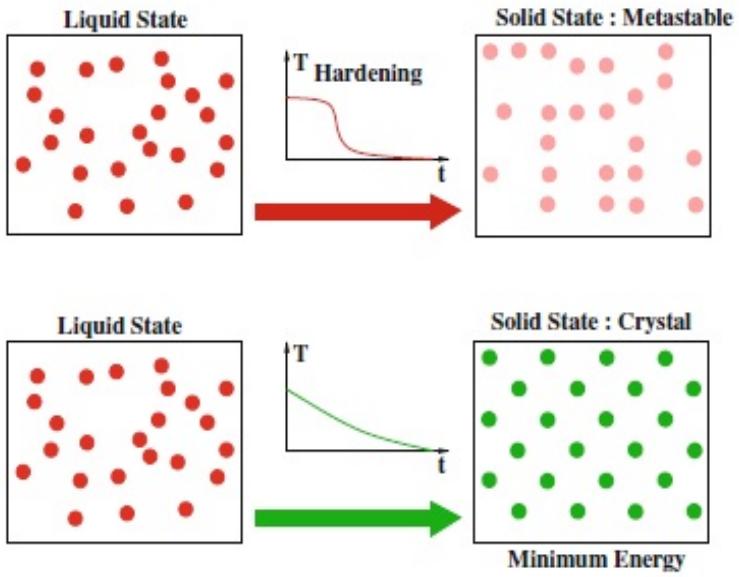

Figure 3.8: Process of Simmulated Annealing

To appreciate the working of simulated annealing, we first need to understand the principles of local search optimization algorithms. SA is just an extension of local search.

A local search algorithm is an iterative algorithm. It starts search from a feasible point randomly drawn in the state space. Algorithm then proceeds with generation of samples to find better solution in the neighbourhood of search space. If better solution is found, it is accepted and becomes the current solution. The algorithm then search for better than current solution. Finally, it ends when no improvement in solution is found. Then, the current solution is accepted as an approximate solution of the optimization problem.

There is a problem with simple local search problem. Local search algorithm converges to local minima, if structure of neighbourhood is not exact. If the current solution falls in a convex subdomain, the solution is trapped in subdomain. In order to being trapped in local minima, it is necessary to accept the solution which momentarily degrade the performance of evaluation function. It is this principle on which simulated annealing is based.

The SA algorithm is based on the assumption that for each point of state space, the neighbourhood and generating a solution in this neighbourhood is defined. The next important point is to define the acceptance principle. The acceptance criterion for accepting solution $\boldsymbol{j}$ against the current solution $\boldsymbol{i}$ is given by the following criterion.

$$P_r\{accept\ \boldsymbol{j}\} = \begin{cases} \{1\ if\ f(\boldsymbol{j})\ <\ f(\boldsymbol{i}) \\ e^{(\frac{f(i)-f(j)}{c})},\ else \end{cases} \tag{3.44}$$

The principle of acceptance is known as Metropolitan Criterion. This algorithm is based on the Monte Carlo Techniques, in which a sequence of solid states is generated in the following way. Starting from an initial state $\boldsymbol{i}$ with energy E_i, a new state $\boldsymbol{j}$ with energy E_j is generated by modifying position of one particle.

If the energy difference $(E_i - E_j)$ is positive, the new state has a lower energy, so the new state $\boldsymbol{j}$ becomes the new current state. If the energy difference is less than or equal to zero, then the probability that the state $\boldsymbol{j}$ becomes the current state is given by

$$P_r\{CurrentState\ =\ j\}\ =\ e^{\frac{(E_i-E_j)}{k_B T}} \tag{3.45}$$

Where $\boldsymbol{T}$ represents the temperature of solid and k_B is the Boltzmann constant (k_B=$1.38 \times 10^{-23}\mathbf{J/K}$). The acceptance criterion of the new state is called the Metropolitan criterion. If the cooling is carried out sufficiently slow, the solid state reaches a state of equilibrium at each given temperature $\boldsymbol{T}$. Using Metropolitan Algorithm, the equilibrium is achieved by generating a large number of transitions at each temperature. A transition is nothing but the replacement of current solution by a neighbouring solution. It is carried out in two stages: generation and acceptance.

3.5.2 Simulated Annealing Process

Simulated Annealing is explained here step-by-step.

1. Initialization ($i = i_{start},\ k\ =\ 0,\ c_k\ =\ c_0,\ L_k\ =\ L_0$)
2. Repeat
3. For $l = 0$ to L_k do

- Generate a solution j from the neighbourhood S_i of current solution i
- $f(j) < f(i)$ then $i = j$ (j becomes the current solution)
- Else, j becomes the current solution with probability $e^{\left(\frac{f(i)-f(j)}{c_k}\right)}$

4. $k = k + 1$
5. Compute (L_k, C_k)
6. $c_k \cong 0$

Where,
c_k is the temperature controlling parameter
L_k is the number of transitions generated at some iterations k
i is the first set of solution

The main feature of SA is its ability to accept transitions even if it degrades the objective function. At the starting of the process, the c_k value is kept high, which makes it possible to accept worst solution with high degradation of objective function and it avoids the problem of stuck-up in local minima and explores the complete space thoroughly. As c_k decreases, only the transition improving the objective or with the low objective deterioration are accepted. Finally, when c_k reaches to zero, the tolerance of acceptance of deteriorated solution is high and possibility of acceptance is negligible.

The simulated annealing algorithm converges asymptotically towards the set of global optimal solutions of the problem. In [327], author has provided a complete proof in their topic Simulated Annealing and Boltzmann Machines: A Stochastic Approach to Combinatorial Optimization and Neural Computing (1989). Essentially, the convergence condition towards global optimum sets that, the temperature $\boldsymbol{T}$ of the system must be decreased logarithmically according to the equation.

An annealing algorithm progresses in three distinct stages; global positioning, local search and refine solution. A cooling strategy should reflect these stages. Any rapid decrement of the temperature would result in a **'quenching'** effect and entrapment of the configuration locally. In the third stage, the temperature decrement rates should be maintained at lower values to result in a flat convergence pattern.

During the middle part of annealing, the algorithm should perform most of the necessary decrements in temperature and settle in the locality of the optimum. During

annealing, the cost function is assumed to follow a Gaussian pattern notably at higher temperatures. Hence a Gaussian-like temperature decrement rule is proposed over the entire annealing process. It is one of the standard cooling temperature reduction, which is logarithmic in nature.

$$T = \frac{T_0}{1 + Log(1+k)} \tag{3.46}$$

3.5.3 Cooling Schedule

A cooling schedule is a temperature decreasing function. A practical simulated annealing implementation requires generating a finite sequence of decreasing value of temperature $\boldsymbol{T}$, and a finite number of state transition $\boldsymbol{L}$ for each temperature value. An appropriate cooling schedule is required to achieve the objectives of optimization. The cooling schedule proposed by Kirkpatrick, Gelatt and Vecchi (1983) [328], is frequently used in various literatures. It has three basic parameters, namely initial temperature ($\boldsymbol{T_o}$), temperature decreasing function and number of state transitions ($\boldsymbol{L}$).

The initial temperature ($\boldsymbol{T_o}$) must be high enough so that the new solution generated is accepted with high probability. In Reference [329],An Efficient Simple Cooling Schedule for Simulated Annealing, a mathematical expression given to find the initial temperature. However, it is entirely user dependent. One can set initial temperature, just enough high so that the ratio of accepted moves to the proposed moves should be nearly equal to 1. The number of state transition ($\boldsymbol{L}$) for each temperature value must be high enough so that it can be ensured that the state space is sufficiently explored.

Temperature decrease function is very important. In practice, the temperature value is reduced to sufficiently small values such that virtually no worse configurations are accepted by the Metropolis acceptance test and no further significant improvement of objective is expected. There are numerous choices about temperature decreasing function. Generally, an exponential decrease function is used, such as, $\boldsymbol{T_k = T_o - \alpha k}$, where $\boldsymbol{\alpha}$ is a constant smaller than the unity. Usual values of $\boldsymbol{\alpha}$ fluctuate between 0.8 and 0.99. The temperature decrease function has been studied in numerous research works (Laarhoven, P.J.M. Van and Aarts, E.H.L., 1987)[330], (Dowsland, K.A., 2001) [331], (Luke, B.T., 2005) [332], (Locatelli, M., 2000) [333]. Mostly, nine different cooling schedules are used in SA algorithm. The nine different cooling schedules are primarily divided in to main

three categories. Namely, Multiplicative Monotonic Cooling, Additive Monotonic Cooling and Non-Monotonic Cooling. The former two are further divided in to four subparts exponential, logarithmical, Linear and Quadratic. Each one is explained here in brief.

3.5.3.1 Multiplicative Monotonic Cooling

In multiplicative monotonic cooling, the initial temperature is multiplied by a factor with every cycle. As discussed, there are four variants of this method.

3.5.3.1.1 Exponential Monotonic Multiplicative Cooling It was proposed by Kirkpatrick, Gelatt and Vecchi (1983) [328]. This method is used as reference in the comparison among the different cooling criteria. The temperature decrease is achieved by multiplying the initial temperature $\boldsymbol{T_o}$ by a factor that decreases exponentially with respect to temperature cycle $\boldsymbol{k}$.

$$T_k = T_0 \cdot \alpha^k \quad (0.8 \leq \alpha \leq 0.9) \tag{3.47}$$

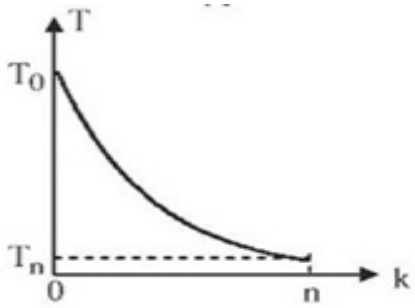

Figure 3.9: Exponential Monotonic Multiplicative Cooling

3.5.3.1.2 Logarithmical multiplicative cooling This method is based on the asymptotical convergence condition of simulated annealing (Aarts, E.H.L. and Korst, J., 1989) [327] by incorporating a factor α. It speed-up the cooling process that makes possible its use in practice. The temperature decrease is achieved by multiplying the initial temperature T_0 by a factor that decreases in inverse proportion to the natural logarithm of temperature cycle k.

$$T_k = \frac{T_0}{1 + \alpha \cdot Log(1+k)} \quad (\alpha \geq 1) \tag{3.48}$$

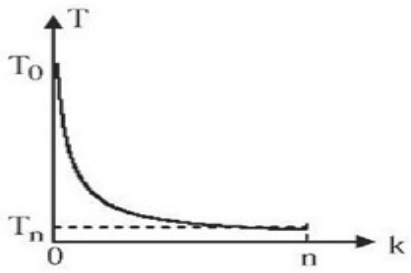

Figure 3.10: Logarithmical Monotonic Multiplicative Cooling

3.5.3.1.3 Linear multiplicative cooling In this method, the temperature decrease is accomplished by multiplying the initial temperature T_0 by a factor that decreases in inverse proportion to the temperature cycle k.

$$T_k = \frac{T_0}{1 + \alpha \cdot k} \quad (\alpha > 0) \tag{3.49}$$

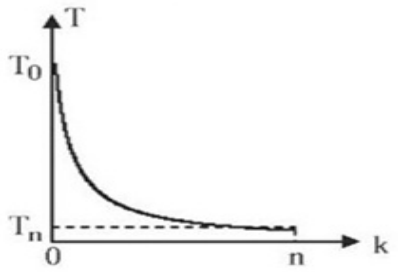

Figure 3.11: Linear Monotonic Multiplicative Cooling

3.5.3.1.4 Quadratic multiplicative cooling The temperature decrease is made by multiplying the initial temperature T_0 by a factor that decreases in inverse proportion to the square of temperature cycle k

$$T_k = \frac{T_0}{1 + \alpha \cdot k^2} \quad (\alpha > 0) \tag{3.50}$$

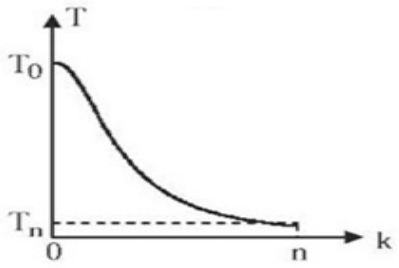

Figure 3.12: Quadratic Monotonic Multiplicative Cooling

3.5.3.2 Additive Monotonic Cooling

In the additive monotonic cooling, two additional parameters are taken in to account, the number n of cooling cycles, and the final temperature T_n of the system. In this type of cooling, the system temperature T at cycle k is computed, by adding to the final temperature T_n, a term that decreases with respect to cycle k. Four variants based on the formulae proposed by B. T. Luke (2005) [332] are considered in practical applications.

3.5.3.2.1 Linear Additive Monotonic cooling In this method, the temperature decrease is achieved by adding to the final temperature T_n, and a term that decreases linearly with respect to temperature cycle k. At n^{th} iteration the second term vanish and T_k becomes equal to T_n.

$$T_k = T_n \ + \ (T_0 - T_n) \left(\frac{n-k}{n}\right) \tag{3.51}$$

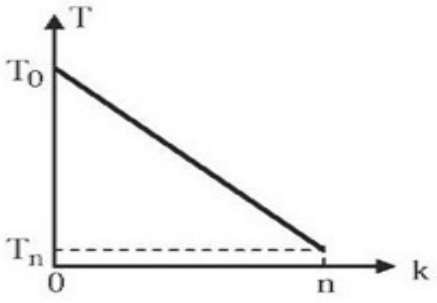

Figure 3.13: Linear Additive Monotonic Cooling

3.5.3.2.2 Quadratic Additive Monotonic cooling In this method, the temperature decrease is achieved by adding to the final temperature T_n a term that decreases in proportion to the square of temperature cycle k.

$$T_k = T_n \ + \ (T_0 - T_n) \left(\frac{n-k}{n}\right)^2 \tag{3.52}$$

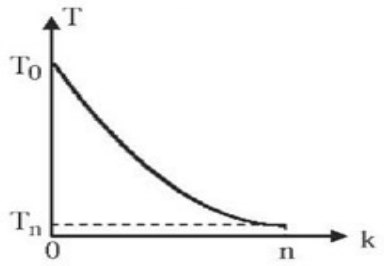

Figure 3.14: Quadratic Additive Monotonic Cooling

3.5.3.2.3 Exponential Additive Monotonic cooling In this method, the temperature decrease is achieved by adding to the final temperature T_n, a term that decreases in inverse proportion to the number raised to the power of temperature cycle k.

$$T_k = T_n \ + \ (T_0 - T_n)\left(\frac{1}{1+e^{\frac{2Ln(T_0-T_n)}{n}\cdot(k-\frac{1}{2}\cdot n)}}\right) \tag{3.53}$$

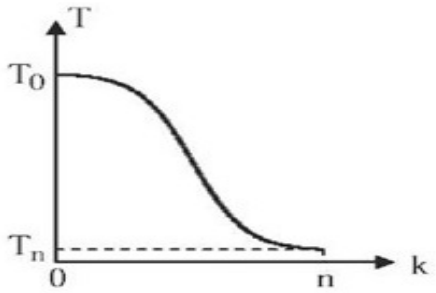

Figure 3.15: Exponential Additive Monotonic Cooling

3.5.3.2.4 Trigonometric Additive Monotonic cooling In this method, the temperature decrease is achieved by adding to the final temperature T_n, a term that decreases in proportion to the cosine of temperature cycle k.

$$T_k = T_n \ + \ \frac{1}{2}(T_0 - T_n)\left(1 + \cos\left(\frac{k\pi}{n}\right)\right) \tag{3.54}$$

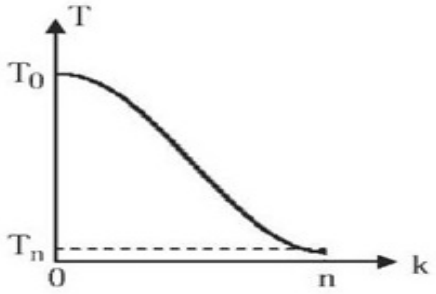

Figure 3.16: Trigonometric Additive Monotonic Cooling

3.5.3.3 Non-Monotonic Adaptive Cooling

In the non-monotonic adaptive cooling, the system temperature T at each state transition is achieved by multiplying the temperature value T_k, obtained by any of the former criteria, by an adaptive factor μ based on the difference between the current solution objective $f(s_i)$, and the best objective achieved until that moment by the algorithm (f^*).

$$T = \mu \cdot T_k = \left(1 + \frac{f(s_i) - f^*}{f(s_i)}\right) T_k \tag{3.55}$$

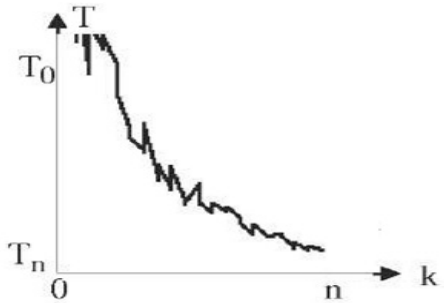

Figure 3.17: Non-Monotonic Cooling

The value of μ should be in the range between 1 & 2. The inequality $1 < \mu < 2$ is not verified here as it has been already done. The factor μ implies that the greater the distance

between current solution and best achieved solution is, the greater the temperature is, and consequently the allowed energy hops/jumps. This criterion is a variant of the one proposed by M. Locatelli (2000) [333], and it can be used in combination with any of the former criteria to compute T_k. In the comparison, the standard exponential multiplicative cooling has been used for this purpose. So the cooling curve is characterized by a fluctuant random behaviour comprised between the exponential curve defined by T_k and its double value $2T_k$

3.5.3.4 Selection of Appropriate Cooling Schedule

In selection of appropriate cooling schedule of simulated algorithm, following points are preferably considered.

1. **Quality of objective with respect to the shape of the temperature decrease curve**: It is affirmed that simulated annealing works properly with respect to the ability of escape from local minima when the curve has a moderate slope at the initial and central parts of the processing, and softer at the final part of it, just as it occurs in the standard exponential multiplicative cooling. The specific shape (convex, sigmoid) of the curve in the initial and central parts does not seem outstanding.

2. **Execution Time**: the standard error of the number of iterations seems to be related to the temperature decrease curve tail at the final part of the algorithm. An inversely logarithmic tail produces a softer final temperature fall and a higher standard error, while inversely quadratic and exponential tails reduces the speed, but provide the best standard error values.

3. **The use of a non-monotonic temperature decrease method**: It is also asserted that not only the utilized criterion does not degrade the general performance of the algorithm but it seems to have a favourable effect that deserves to be taken into account and studied in greater depth.

3.5.3.5 Objective Function Formulation

To achieve the overall best results, filter optimization is carried out. In this part, different types of filters are considered. Each type of filter is connected at different buses and optimization is done using Simulated Annealing with linear multiplicative cooling schedule. The objective of the optimization is to reduce the overall Modal impedance. It is achieved by formulating objective function as given below.

$$Z_m = \sqrt{\frac{\sum_{j=1}^{N}\sum_{i=1}^{n} Z_{ij}^2}{N}} \tag{3.56}$$

Where, Z_{ij} = Modal Impedance n= Number of Modes N = Total number of Frequency data points. Here it is considered up to 200^{th} order in steps of 0.1 Hz.

Also, the filter parameters are subject to fillowing constraints

$$C_{min} < C_{filter} < C_{max} \tag{3.57}$$

$$L_{min} < L_{filter} < L_{max} \tag{3.58}$$

$$R_{min} < R_{filter} < R_{max} \tag{3.59}$$

$$Z_n < Z_{max} \tag{3.60}$$

The value of capcitor is derived from overall reactive power requirement that can be accomodated in the system without affecting voltage. The inductance value is then derived from the resonant point. The damping resistor is then calculated from the quality factor requirement of filter. The max value of impedance Z_{max} is important to rule out violation of harmonic limits. Its value should be such that $I_h \times Z_{max} < V_{h_{limit}}$. Where, $V_{h_{limit}}$ is the allowable harmonic voltage distortion at respective voltage level as per IEEE 519-1992 / 2014.

3.6 Description of Test Network

Integration of Wind Farms to the power system has some challenges, one of them is the harmonic resonance or harmonic magnification. Several tripping has been observed in the recent days in Wind Farms. Connecting inverters to the grid requires assessment of network impedance and also of behaviour of network impedance to change in frequency. Direct connection of inverters to the grid may give rise to PQ problems. The layout of wind farms are depends on how wind turbines are arranged and connected to the collector. The impedance of wind farm varies with the change in the network structure and addition or removal of inductive and capacitive elements to the grid. One such model farm is shown here in figure 3.18. This network taken here for study is based on the typical layout of wind power plant discussed in reference ([334]) and actual layout of Wind Farm located in coastal area of Porbandar, Gujarat given in reference [335]. However, some modifications are made to make it more general. Actually, the wind turbine connected to pooling station transformer through cable, which is different for different wind turbines, but here it is assumed uniform cable length for sake of simplicity in analysis. The wind farm under study consists of 60 WT of 2 MW each. The total aggregate capacity of the wind farm is 120 MW. Each WT is connected to the 0.44 /1.1 KV Transformer. At wind turbine terminal 200 kVAr, 0.440 kV capacitor is connected for power factor improvement. Five WT, each of 2 MW, are connected on each 1.1 kV Bus. From 1.1 kV Bus the voltage level is first raised to 33 kV and then tramsmitted to 33 kV Collector bus through 33 kV cable, which is of 1 km length. On 33 kV bus such 6 groups of WT are connected. So the total capacity on each 33 kV bus is 60 MW. There are two such 33 kV collector bus. The power is then evacuated using 33/132 kV power transformer and then feed to the grid using 132 kV transmission line. The network diagram and value of network parameters are given here.

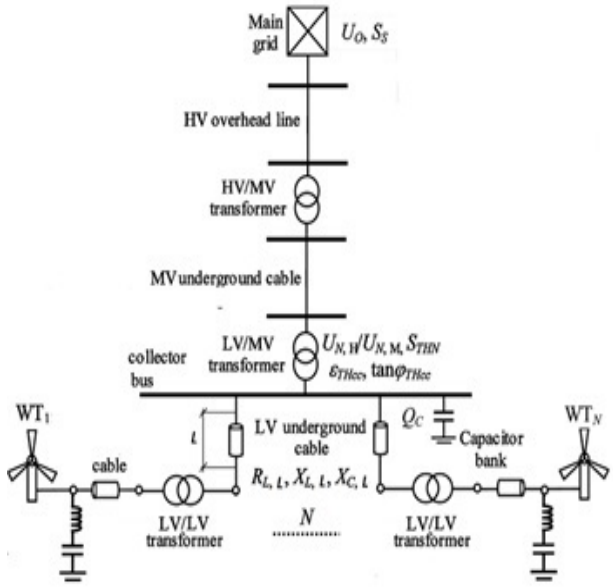

Figure 3.18: Wind Farm Network

The network with passive elements is shown in figure (3.19) and the aggregated network is shown in figure (3.20)

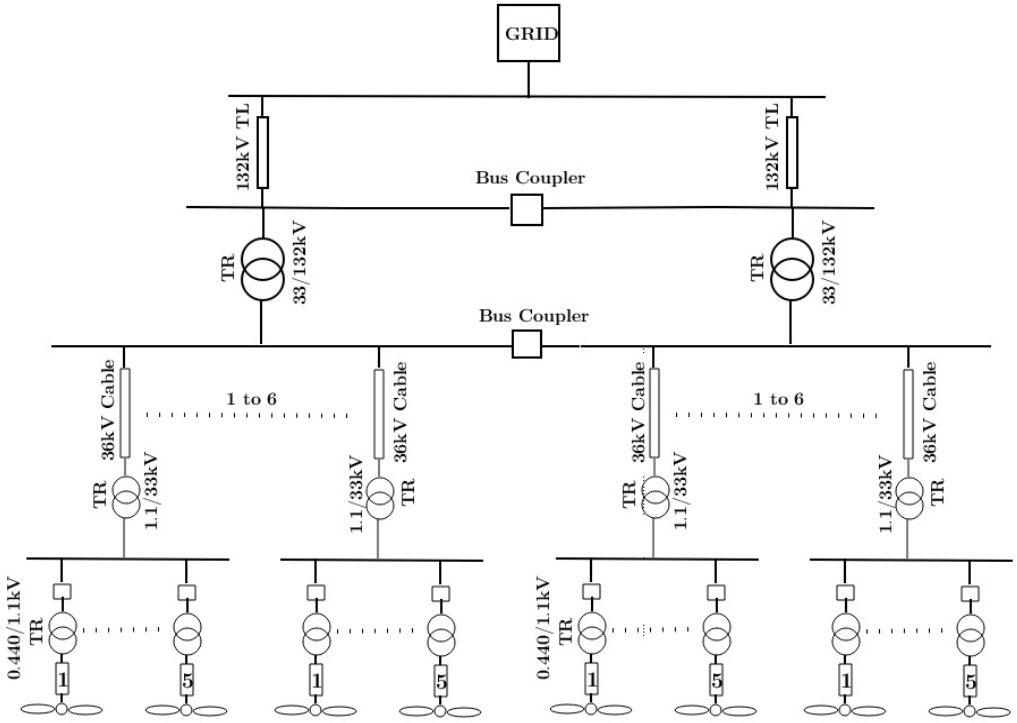

Figure 3.19: Detailed Wind Farm Network

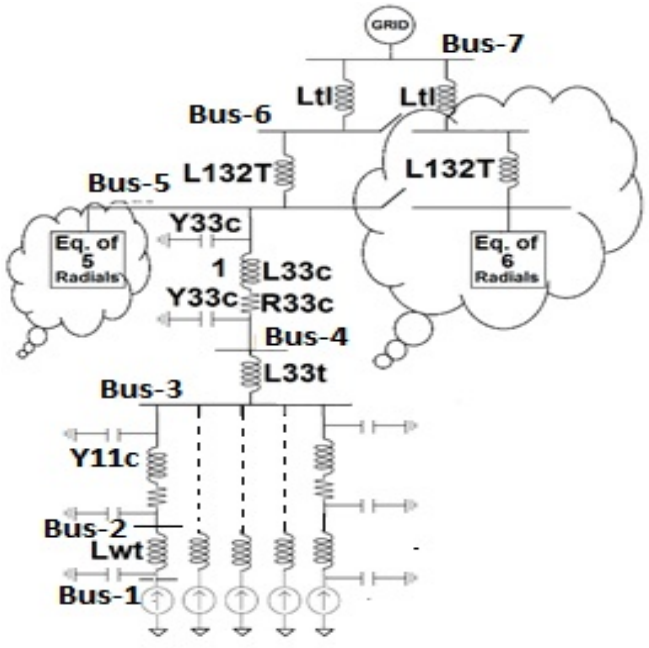

Figure 3.20: Aggregated Wind Farm Network

Table 3.2: Network Parameter

Sr. No	Element	Value reffered to 33 kV	Description
1	Y_{cb}	$\imath 184e^{-6}$	PF Capacitor
2	X_{DR}	$\imath 381.5$	7% Detuned Reactor
3	X_{11t}	$\imath 43.56$	$0.44/1.1kV$ 2 MVA Transformer
4	Z_{11c}	$9 + \imath 18$	1.1 kV Cable
5	Y_{11c}	$\imath 1.25e^{-7}$	1.1 kV Cable
6	X_{33t}	$\imath 8.712$	$1.1/33V$ 10 MVA Transformer
7	Z_{33c}	$0.47 + \imath 1.6$	33 kV Cable
8	Y_{33c}	$\imath 113.1e^{-6}$	33 kV Cable
9	X_{132t}	$\imath 0.363$	$33/132kV$ 60 MVA Transformer
10	Z_{132tl}	$5e^{-5} + \imath 9.045e^{-4}$	132 kV Transmission Line
11	Z_g	$0.0241 + \imath 0.4347$	Grid Impedance

3.7 Results and Discussion

3.7.1 Modal Analysis of Wind Farm Connected to Power System

First, Y matrix is formed and then critical modes are found out using eigenvalue analysis. After evaluation of result, three critical modes are identified. These modes are 3, 4 and 5 respectively. The mode 3 has two peaks, which shows the effect of network aggregation. Three critical modes are observed which indicates the high impedance offered by network at three different frequencies. These frequencies can be considered as critical frequencies due to their magnitude. Apart from this, some non-critical modes are also observed, these are mode-1, mode-2, mode-6 and mode-7. The first observed critical mode is mode - 3. It has two critical frequencies, first at 9.4^{th} order and second at 47.9^{th} order. Both frequencies can affect the WTG stability. Figure (3.21) shows the mode-3 and figure (3.22) and (3.23) shows the expanded view of mode-3. It is important to known that there are small ripples observed in figure (3.21), these are small peaks due to the aggregation of network, which contains system inductances and presence of several capacitive elements in the network.

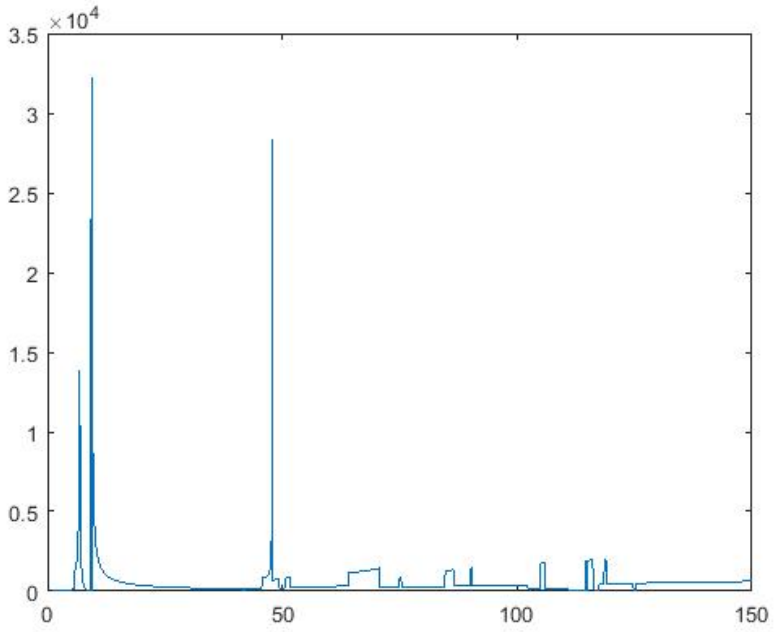

Figure 3.21: Mode-3 of Wind Farm

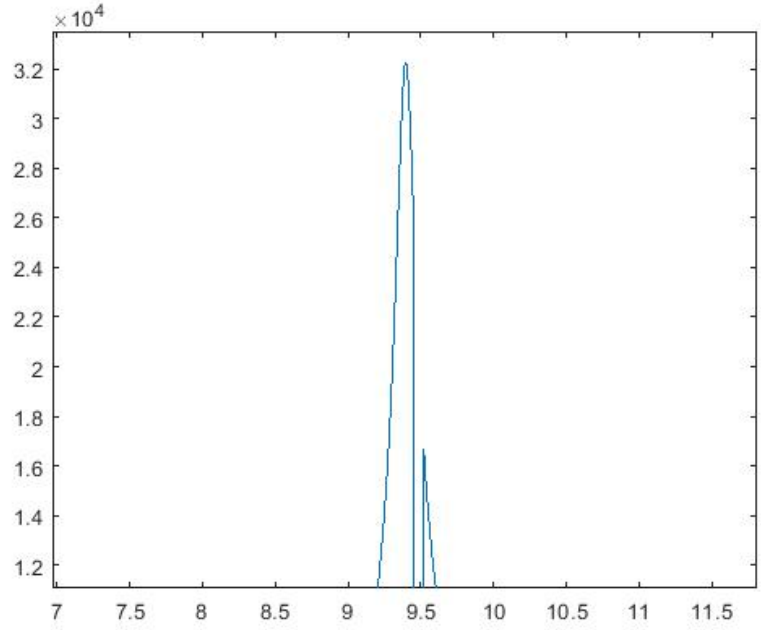

Figure 3.22: First peak of Mode- at 9.4^{th} order

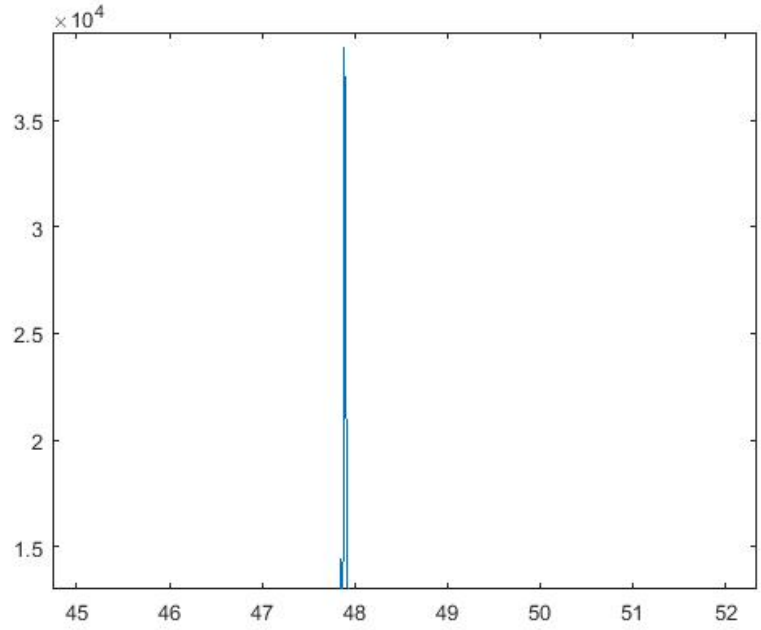

Figure 3.23: Second peak of Mode-3 at 47.9^{th} order

The participation factor for mode-3 is given in table (3.3)

Table 3.3: Participation Factor of Mode -3

	9.4^{th} Mode-3-1	47.9^{th} Mode-3-2
Bus-1	0.8458	0
Bus-2	0.1343	0.1552
Bus-3	0.0191	0.3126
Bus-4	0	0.3883
Bus-5	0	0.1430
Bus-6	0	0
Bus-7	0	0

To verify the trueness of the result, the critical resonance frequencies are verified by analytical method. As per participation factor given in table (3.3), Bus 1,2 and 3 are participating in first peak of mode -3. The elements connected to Bus 1,2 and 3 are shown in figure 3.24. Analytical expression for peak-1 of Mode-3 is given by equation 3.61. This is near to the first peak of mode-3 at 9.4^{th} order.

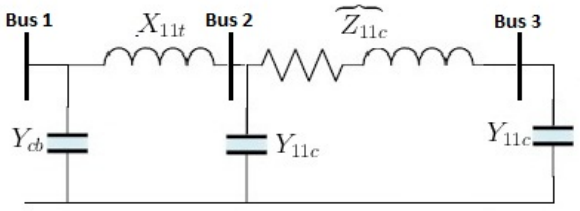

Figure 3.24: Part of Network Participating in Mode-3-1 at 9.4^{th} order

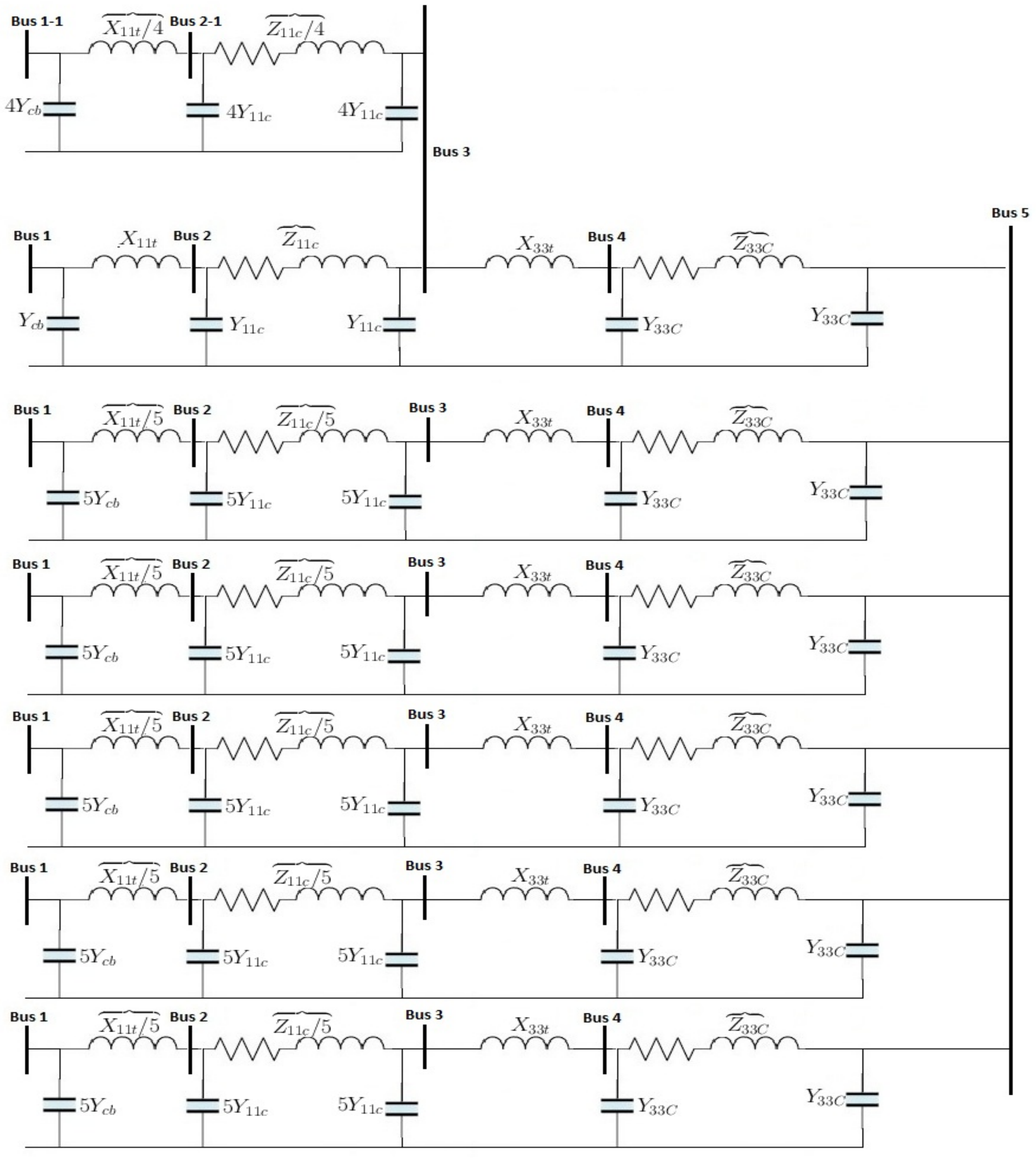

Figure 3.25: Part of Network Participating in Mode-3-2 at 47.9^{th} order

$$\sqrt{\frac{Z_{cb}}{X_{11t} + Z_{11c}}} = 9.4 \tag{3.61}$$

As per the participation factor for mode-3, it can be concluded that the main contributors to peak -1 of mode-3 are, the power factor correction capacitor, reactance of

0.4/1.1 kV Transformer and 1.1 kV cable impedance. In order to control this mode, associated components should be modified. Also, it is to be noted that, with the change in reactive power compensation at wind turbine terminal, this mode also get shifted to a new critical frequency and keeps on changing with level of compensation. Similarly, mode-4 and mode-5 contributed by other elements of the network is given here with their participation factor. Mode-4 is observed at critical frequency of 76^{th} order and mode-5 is at 32.5^{th} order.

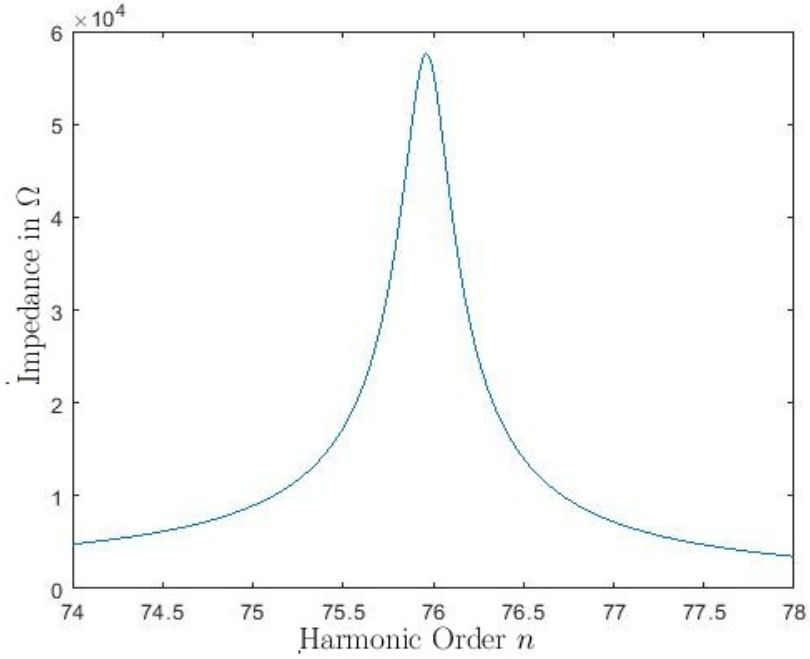

Figure 3.26: Mode-4 at 76^{th} order

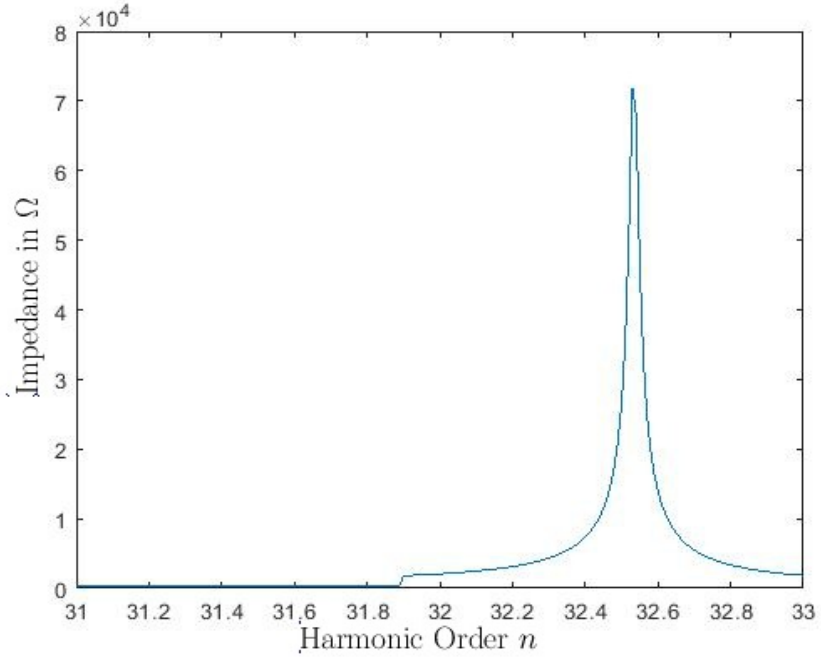

Figure 3.27: Mode-5 at 32.5^{th} order

Table 3.4: Participation Factor of Mode 4 and 5

	76^{th} Mode-4-1	32.5^{th} Mode-5-1
Bus-1	0	0
Bus-2	0.1886	0.1076
Bus-3	0.3727	0.2247
Bus-4	0.4410	0.2863
Bus-5	0	0.1962
Bus-6	0	0.0917
Bus-7	0	0.0915

The result of Modal analysis is very crucial for harmonic resonance mitigation point of view. Peak-1 of mode-3 is local mode and it mainly affect the Bus-1 as the participation factor PF_{13} is very high as compared to other participation factor. The peak-2 i.e 47.5^{th} order, is affecting mainly bus-3 and bus-4. The mode-4 is observable at bus-3 and bus-4,

whereas mode-5 is affecting all the buses more or less except bus-1. The harmonic mitigation is effective where the harmonics are observable and controllable. So, the effective locations can be decided by calculating the participation factor for each mode.

There are some non-critical frequencies or frequencies where relatively lower Modal impedance are observed. The other non-critical modes are given here. The mode-1,2,6 and 7 are non critical mode as their amplitude is not as high as critical mode. Also, modes 3, 4 and 5 has some frequencies, where the Modal impedance is not very high but moderately high. This non-critical frequencies can affect the system when amplitude of current at resonance frequencies are significantly high. The non-critical modes and their Bus Participation are given here.

Table 3.5: Participation Factor of Mode 1 and 2

	125^{th} Mode-1	$50^{th} - 65^{th}$ Mode-2-1	$92^{th} - 102^{th}$ Mode-2-2	$120^{th} - 150^{th}$ Mode-2-3
Bus-1	0	0	0	0
Bus-2	0.8115	0.7322	0.8449	0.7982
Bus-3	0.1855	0.2527	0.1456	0.2001
Bus-4	0.0028	0.0127	0.0092	0.0016
Bus-5	0	0.0013	0	0
Bus-6	0	0	0	0
Bus-7	0	0	0	0

Table 3.6: Participation Factor of Mode 3, 4 and 5

	73^{th} Mode-3-3	$102^{th} - 118^{th}$ Mode-4-2 (108)	$65^{th} - 120^{th}$ Mode-5-2 (110)
Bus-1	0	0	0
Bus-2	0.3698	0.8043	0.1802
Bus-3	0.3924	0.1905	0.2335
Bus-4	0.2371	0	0.1716
Bus-5	0	0.0027	0.2634
Bus-6	0	0	0.1236
Bus-7	0	0	0.1233

Table 3.7: Participation Factor of Mode 6

	$32^{th} - 44^{th}$ Mode-6-1 (33.3)	$109^{th} - 111^{th}$ Mode-6-2 (110)	117^{th} Mode-6-3	113^{th} Mode-6-4
Bus-1	0	0	0	0
Bus-2	0.033	0.7597	0.2434	0.1741
Bus-3	0.1376	0.0430	0.2074	0.8095
Bus-4	0.3141	0.0931	0.1737	0.0147
Bus-5	0.2612	0.1001	0.4763	0
Bus-6	0.1268	0.0493	0	0
Bus-7	0.1266	0.0492	0	0

Table 3.8: Participation Factor of Mode 7

	41.8^{th} Mode-7-1	113.3^{th} Mode-7-2
Bus-1	0.0032	0
Bus-2	0.7306	0.8241
Bus-3	0.2514	0.1710
Bus-4	0.0133	0.0043
Bus-5	0	0
Bus-6	0	0
Bus-7	0	0

Bus-1 and Bus-2 are participating in peak -1 of mode - 3 at 9.4^{th} order. It is due to the parallel resonance of power factor capacitor connected at wind turbine terminal at 0.440 kV and the reactance of 0.440/1.1 transformer. To suppress or shift this mode, changes in participating parameters should be attempted. It is obvious that transformer reactance cannot be changed, but the topology of power factor capacitor can be modified by converting it in to a filter. The peak-2 of mode-3 is observed at 47.9^{th} order. As per the participation factor, this peak is observable at bus 2,3,4 and 5. So, it is obvious that, this mode is controllable from these buses only. In contrast to peak-1 of mode-3, peak - 2 is distributed, as it is observed at multiple buses. So, it can be controlled from these buses only. In this case, it is difficult to decide best place to install filter. The similar argument is valid for Peak-1 of mode-4 and Peak-1 of mode-5. Mode-4 is more or less localized and mode-5 is distributed. So, mode-5 is difficult to control as compared to mode-4. The majority of non-critical modes are distributed in nature. So, this modes should be controlled after careful evaluation.

3.7.2 Detune Reactor on PF Capacitor

Peak-1 of mode-3 at 9.4^{th} order should be attempted to mitigate because this is a lower order harmonics and near to the fundamental frequency as compared to other high order harmonics. In fact, this is the smallest significant harmonic mode. Bus-1 and Bus-2

participate in this mode. So, it is definitely can be controlled from this buses. Bus-1 has the highest participation factor. Thus, by modifying power factor capacitor, connected to Bus-1, peak-1 of mode-3 can be controlled. In industries, it is standard practice to use detuned reactor in capacitor bank to avoid resonance problem. There are various options about the rating of detuned reactors. The more popular are 7% and 14% detuned reactor. A 14% reactor is generally used for avoiding 3^{rd} order harmonic resonance. But, here the first mode is occurring at 9.4^{th}, which is above 3^{rd} order, so 7% detuned reactor is sufficient to modify mode-3. A 7% detuned (Anti-resonant) reactor is added in series with the 200 kVAr capacitor and then Modal analysis is carried out. The results of with detuned reactor is compared with results of network without detuned reactor. It is given in figure (3.28) to (3.41)

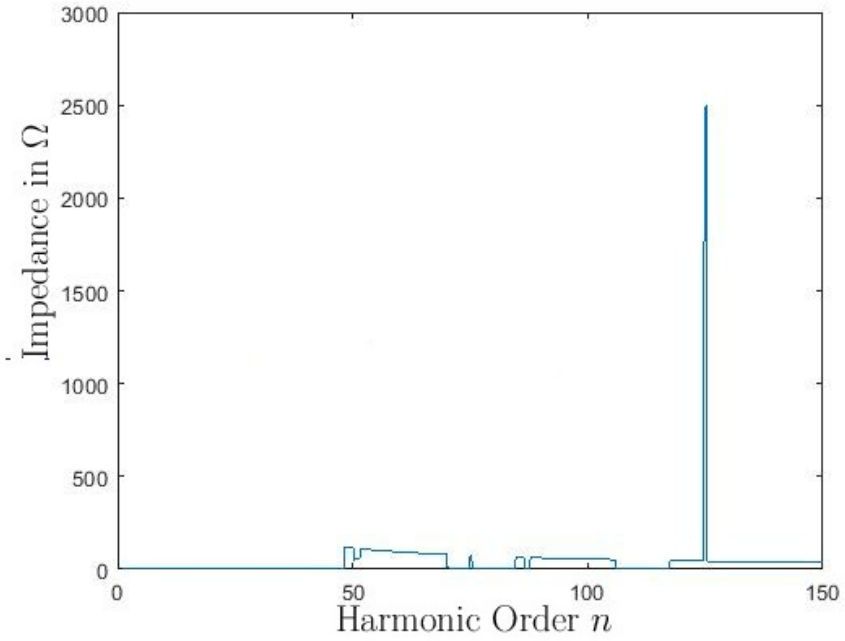

Figure 3.28: Mode-1 without Detuned reactor

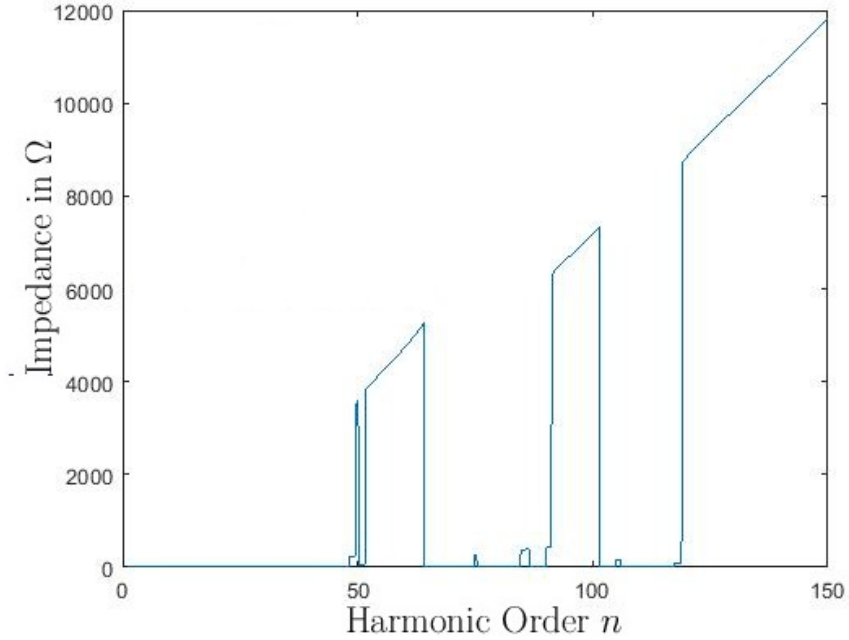

Figure 3.29: Mode-1 with Detuned reactor

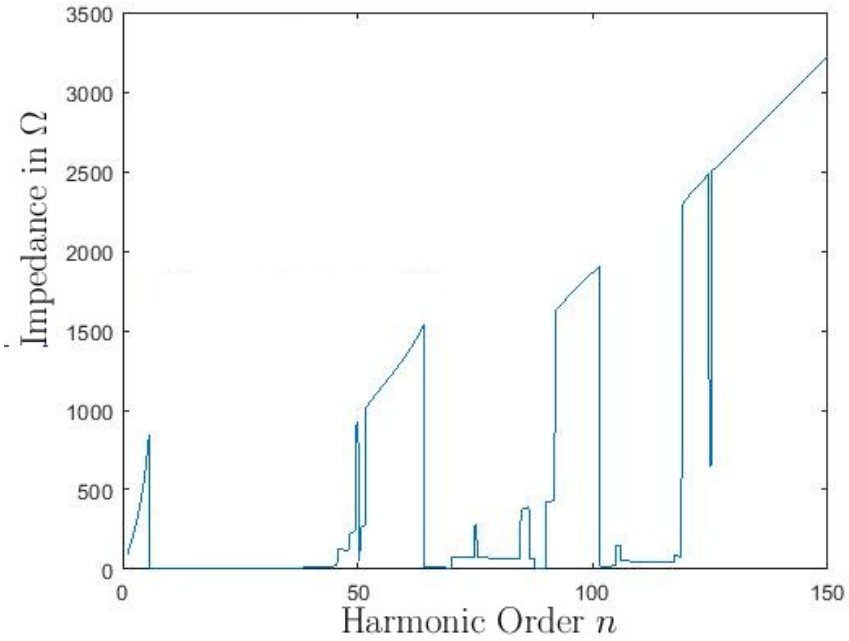

Figure 3.30: Mode-2 without Detuned reactor

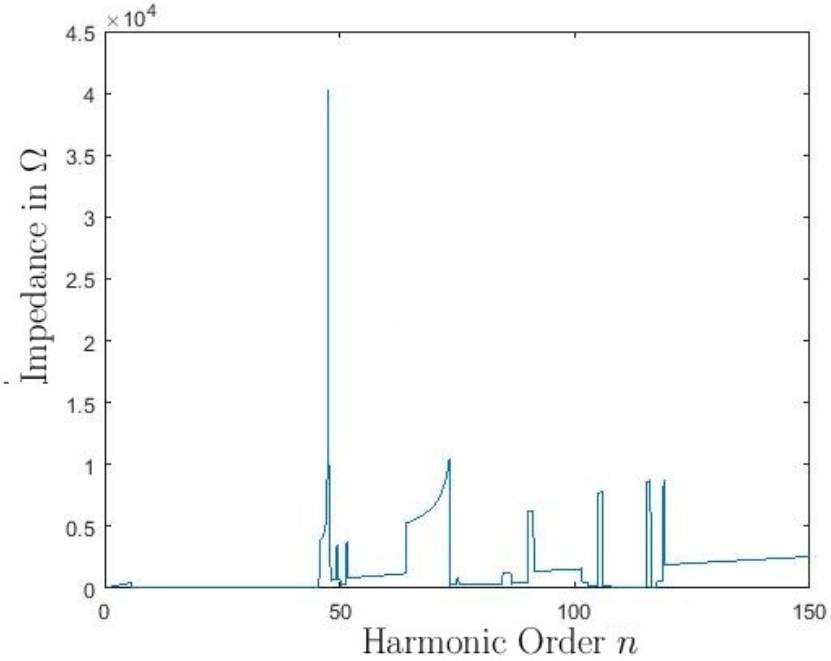

Figure 3.31: Mode-2 with Detuned reactor

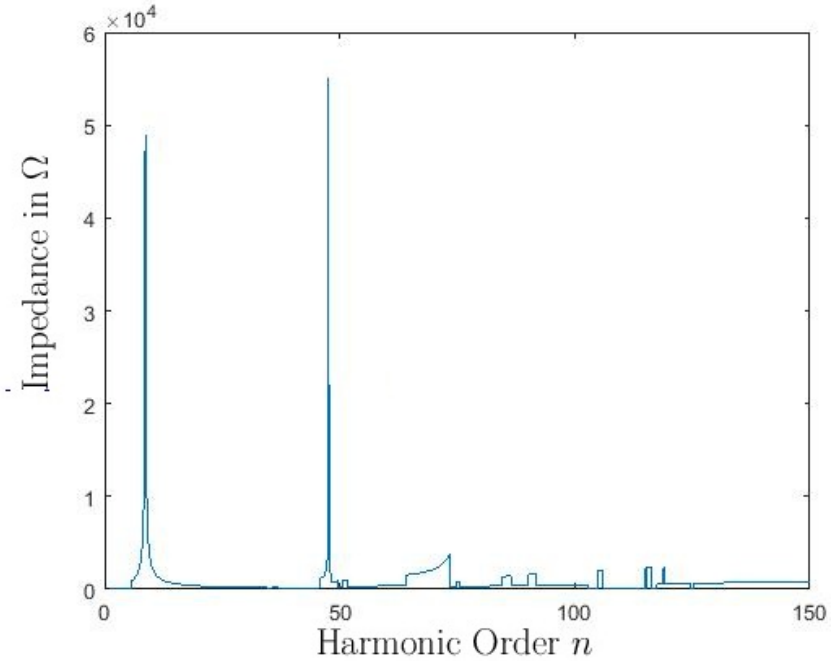

Figure 3.32: Mode-3 without Detuned reactor

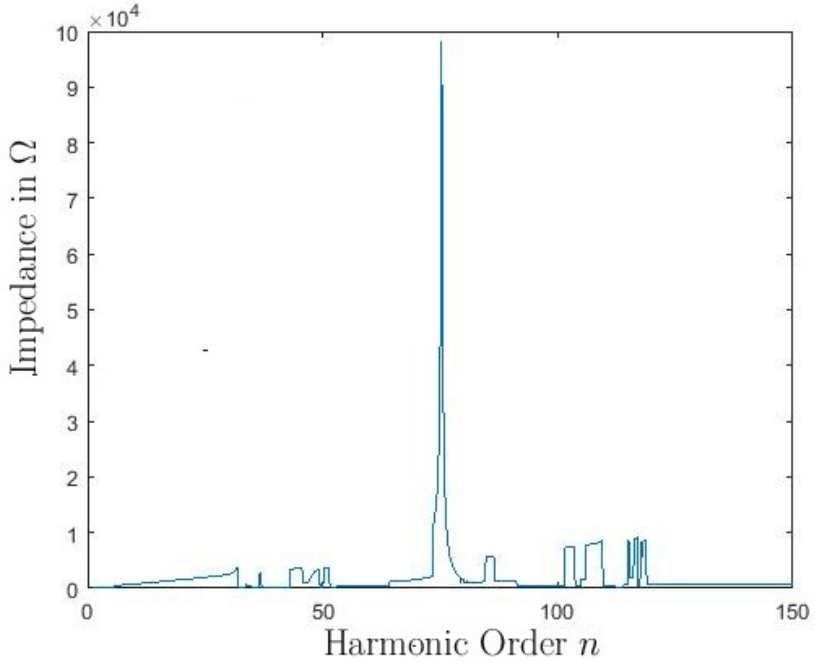

Figure 3.33: Mode-3 with Detuned reactor

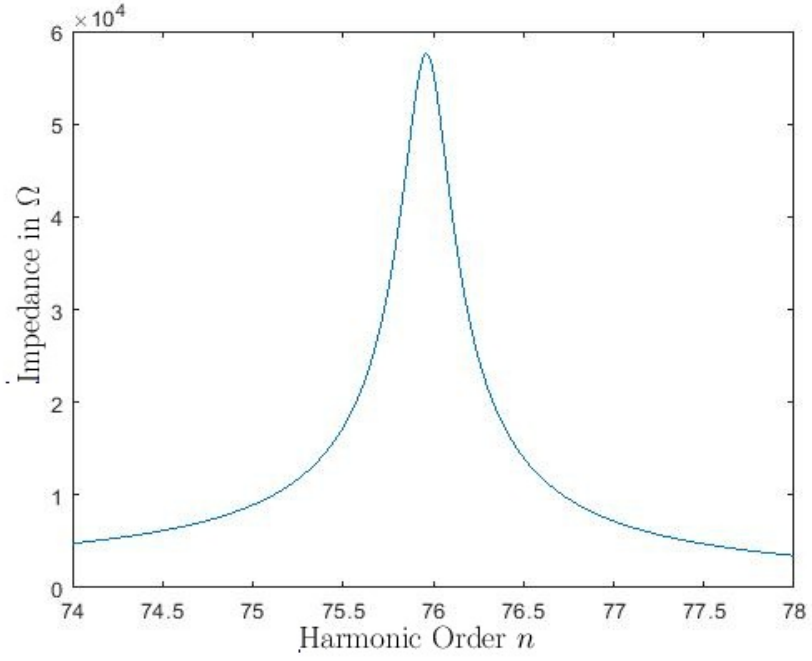

Figure 3.34: Mode-4 without Detuned reactor

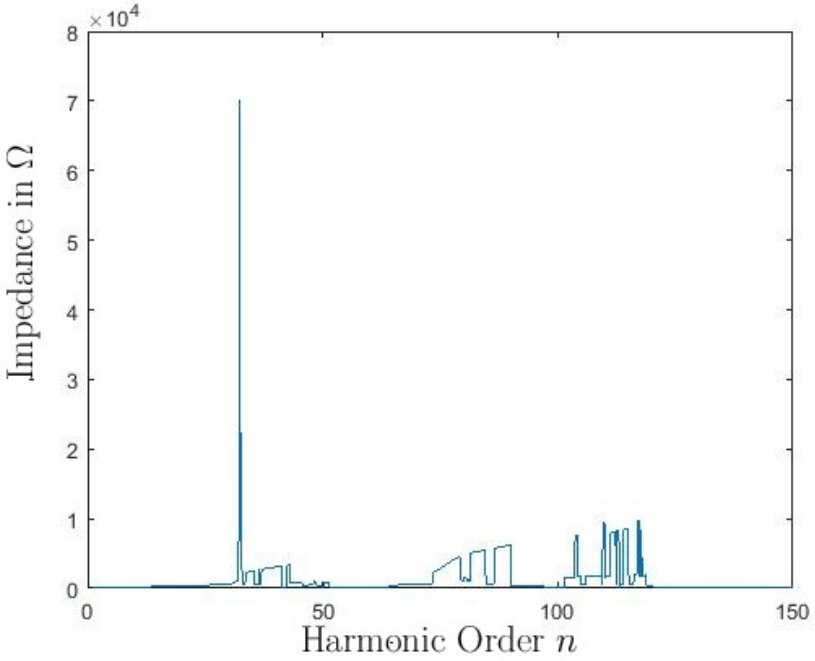

Figure 3.35: Mode-4 with Detuned reactor

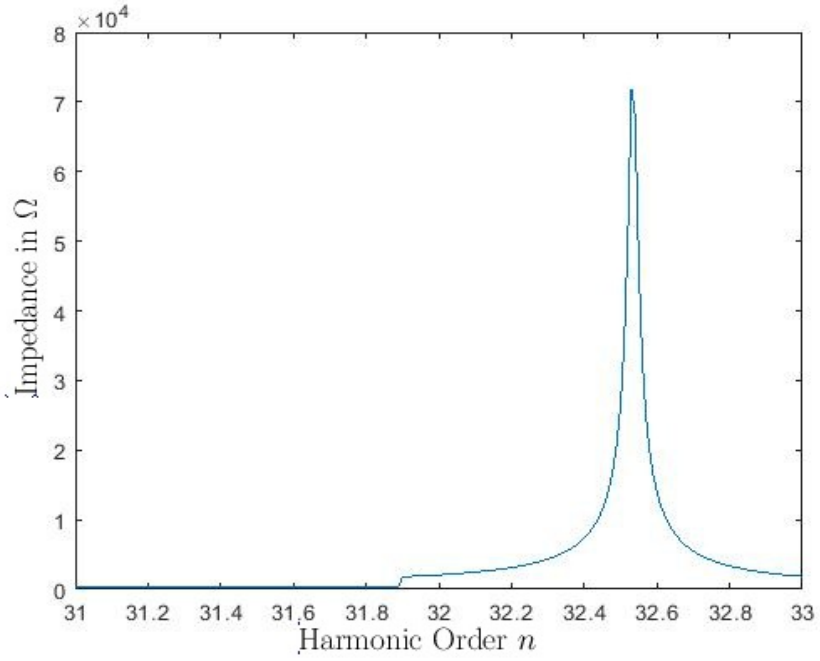

Figure 3.36: Mode-5 without Detuned reactor

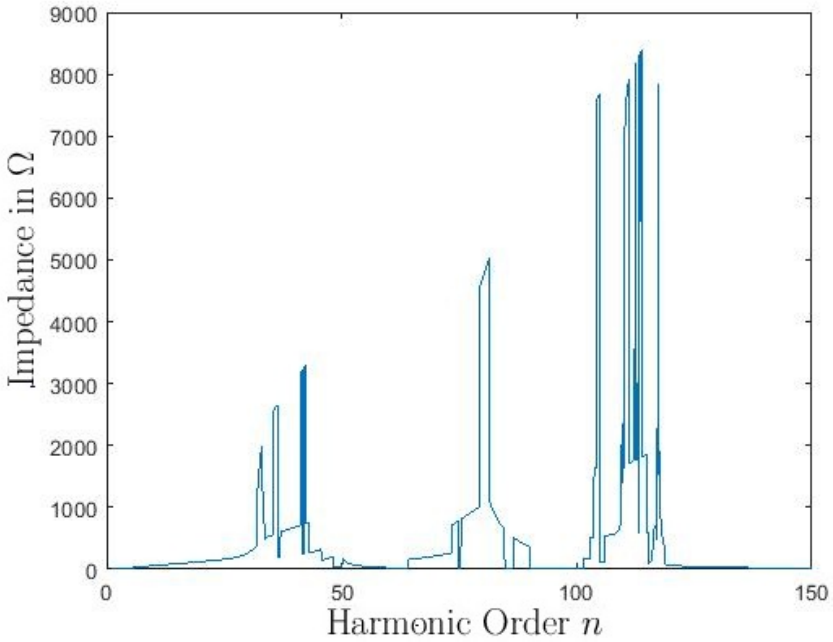

Figure 3.37: Mode-5 with Detuned reactor

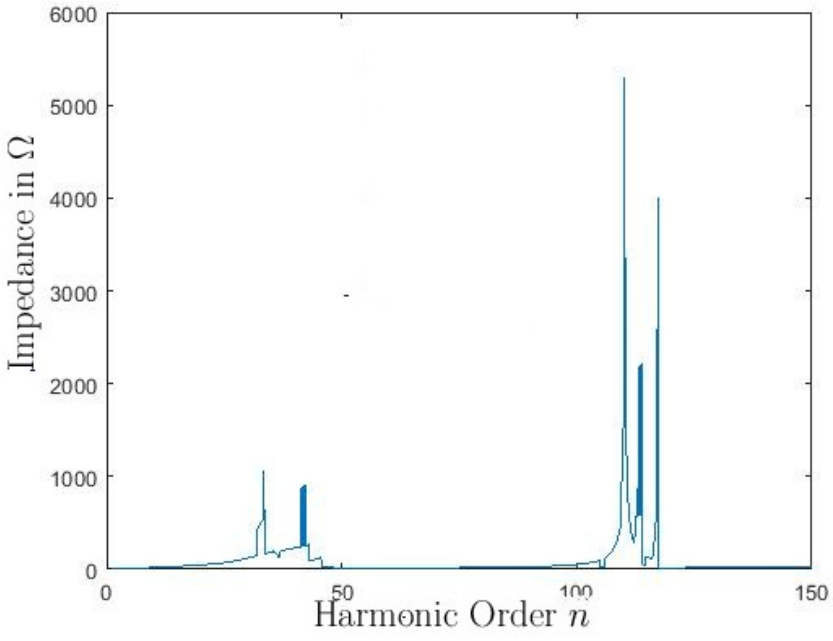

Figure 3.38: Mode-6 without Detuned reactor

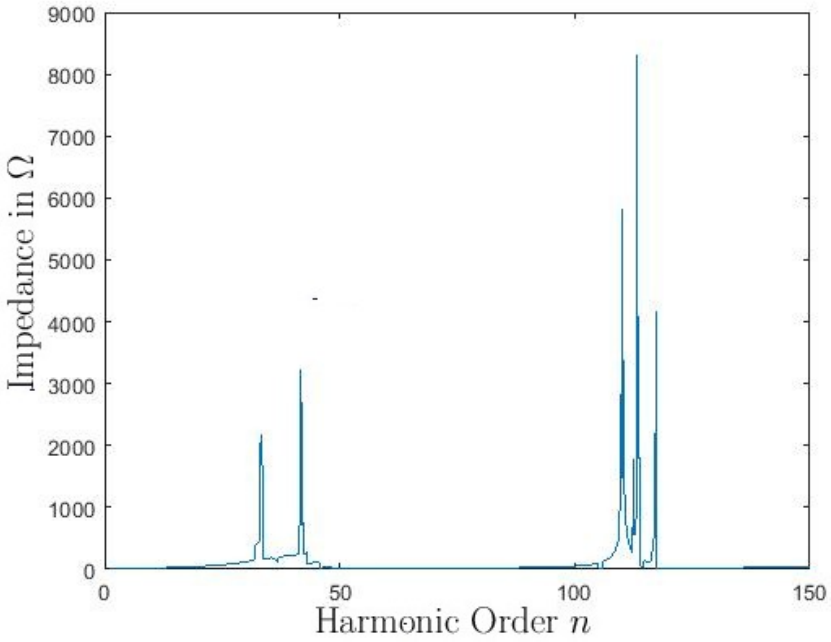

Figure 3.39: Mode-6 with Detuned reactor

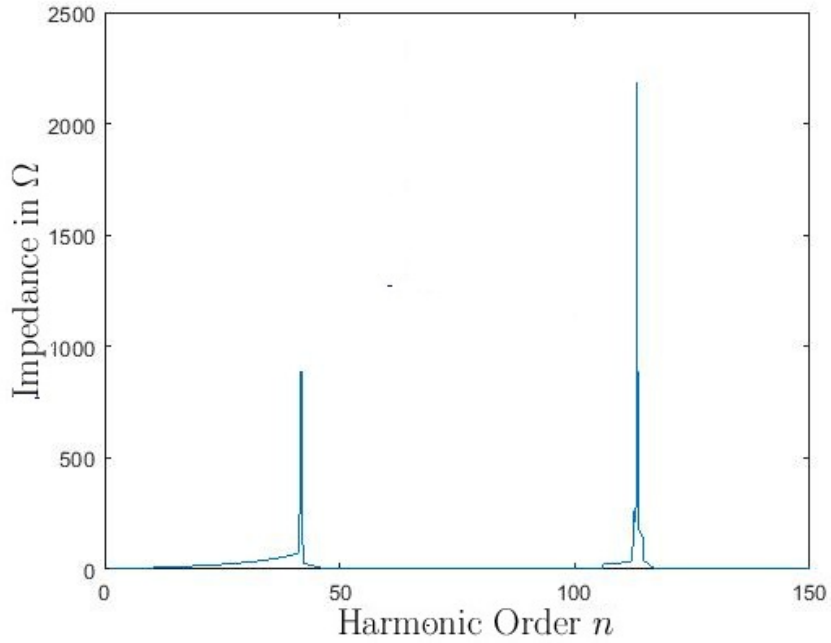

Figure 3.40: Mode-7 without Detuned reactor

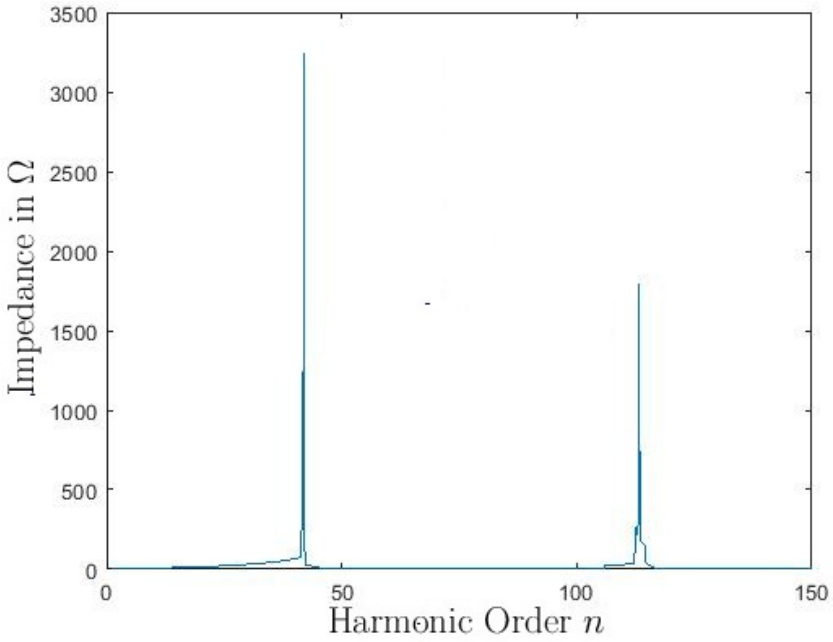

Figure 3.41: Mode-7 with Detuned reactor

Inclusion of detuned reactor suppress the peak-1 of mode-3 at 9.4^{th} order. The other modes remain, more or less, unaffected. One more observation is about the slight shift in resonant frequency. The result of Modal analysis is compared in table (3.9). The result reveals that the mode ranging from 30^{th} to 150^{th} order. This modes are distributed, i.e. produced by several elements of network connected to different buses, so different buses are participating in these modes. Distributed modes are difficult to suppress as compared to localised or concentrated mode, which are restricted to one or two buses. Careful examination of participation factors and associated elements are required for suppression of distributed modes.

Table 3.9: Comparison of Modal Analysis with and without detuned reactor

	Mode Order without Detuned Reactor	Mode Order with Detuned Reactor on 200 kVAr Capacitor
Mode-1	125	Multiple (< 50)
Mode-2	Multiple (< 50)	47.5
Mode-3	9.4, 47.9	75.5
Mode-4	76	32.5
Mode-5	32.5	Multiple (30 to 125)
Mode-6	33, 41.5, 42.5, 111, 113, 117	32.5, 42.5, 110, 112, 113, 117
Mode-7	42, 113	42, 113

The comparison of result of Modal analysis shows that, the inclusion of detuned reactor on PF capacitor modifies the concerned mode (9.4 Hz) only, which is targeted. The other modes remain more or less the same. This is very important conclusion drawn from the result of Modal analysis after inclusion of detuned reactor.

3.7.3 Modal Analysis with Detuned Reactor and C-Type Filter on Bus-5

To mitigate the harmonics, C type filter has been installed at Bus-5. The result of Modal analysis of network with detuned reactor on 200 kVAr PF Capacitor and 15 MVAr of C-type filter on Bus-5 is compared with the Modal analysis of bare network i.e. without any compensation. The rating of filter is based on the steady state reactive power required to uplift the power factor from 0.97 to 0.999. The results are given in figure 3.43 to 3.49. Also the results are compared in table 3.11

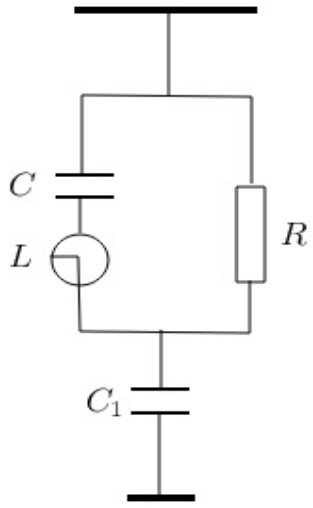

Figure 3.42: C - Type Filter

Table 3.10: C Type Filter Parameters

C-Type Filter	
C1	$40\mu F$
C	$36 \times 10^3 \mu F$
L	$0.2811mH$
R	50Ω

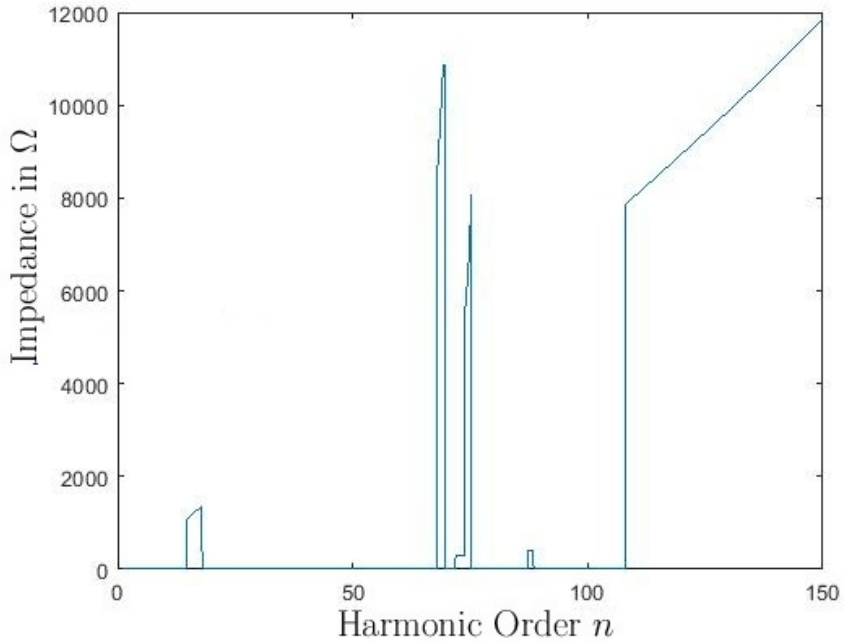

Figure 3.43: Mode-1 with Detuned Reactor and C Filter on Bus-5

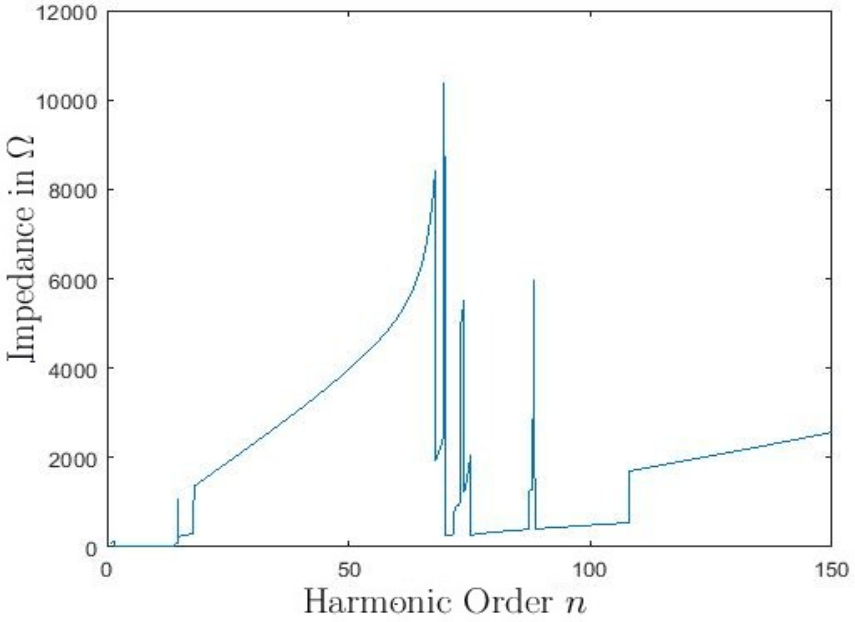

Figure 3.44: Mode-2 with Detuned Reactor and C Filter on Bus-5

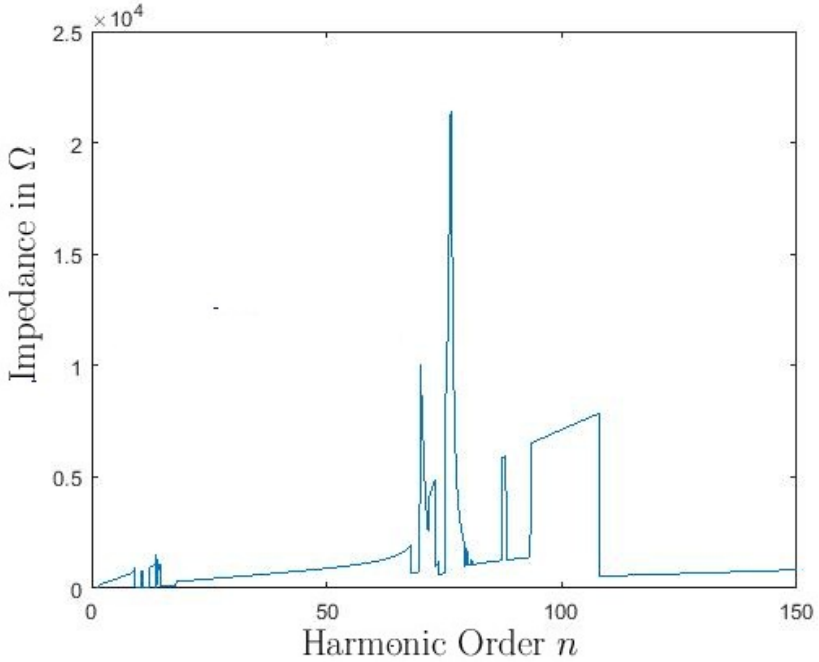

Figure 3.45: Mode-3 with Detuned Reactor and C Filter on Bus-5

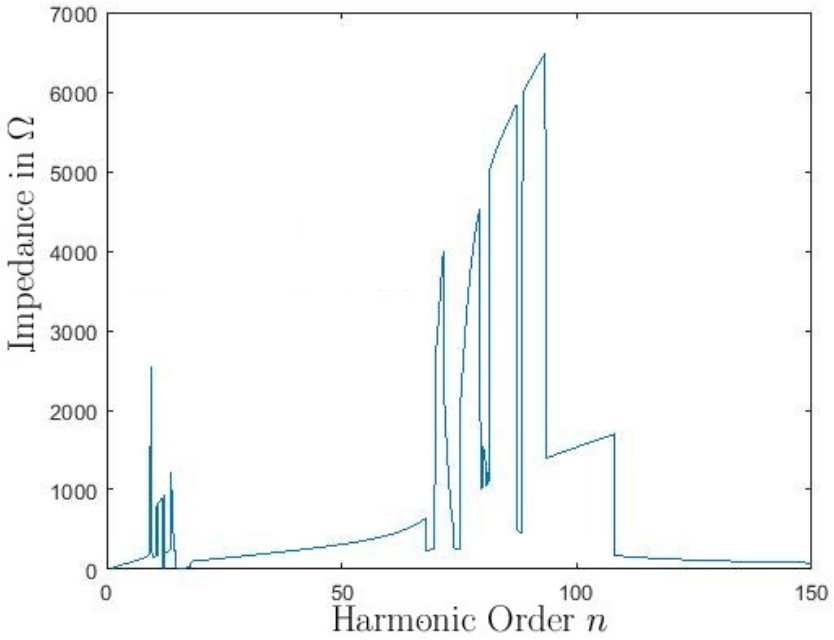

Figure 3.46: Mode-4 with Detuned Reactor and C Filter on Bus-5

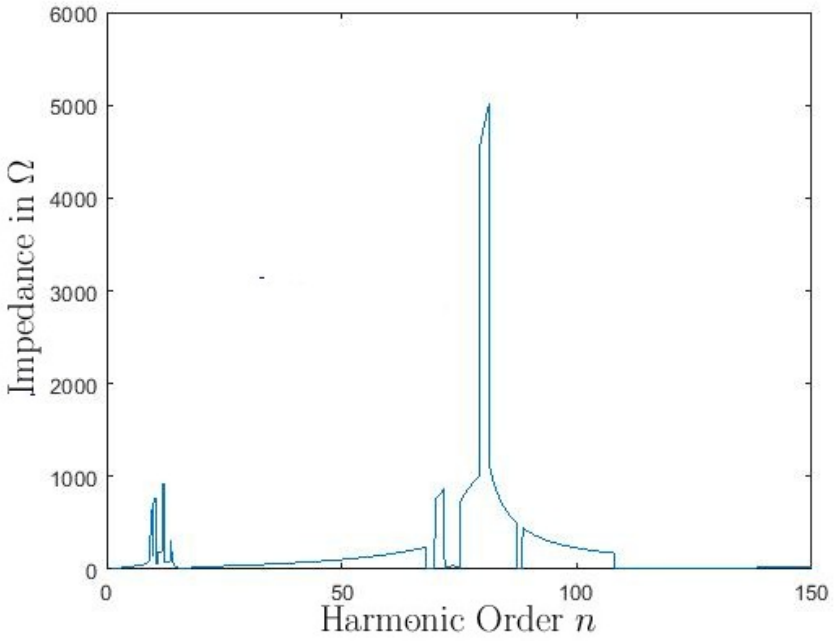

Figure 3.47: Mode-5 with Detuned Reactor and C Filter on Bus-5

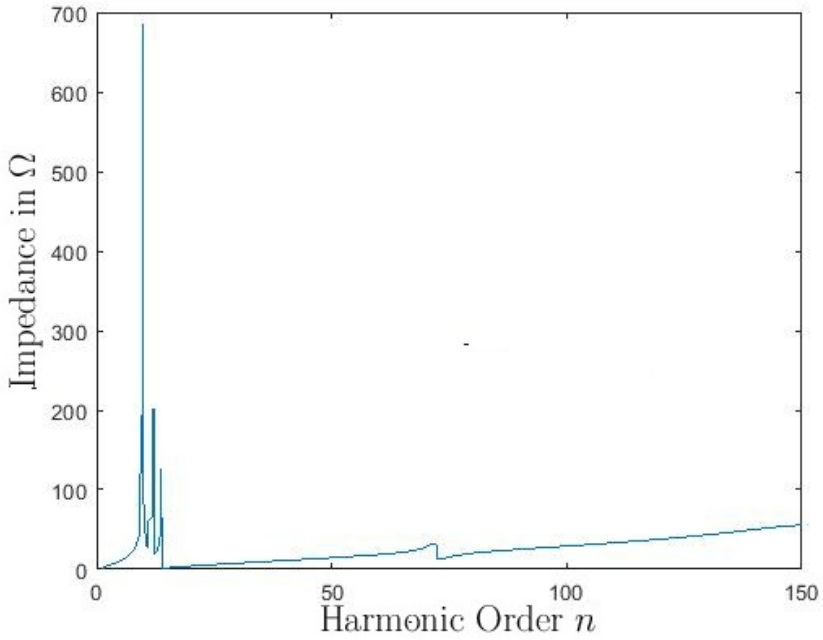

Figure 3.48: Mode-6 with Detuned Reactor and C Filter on Bus-5

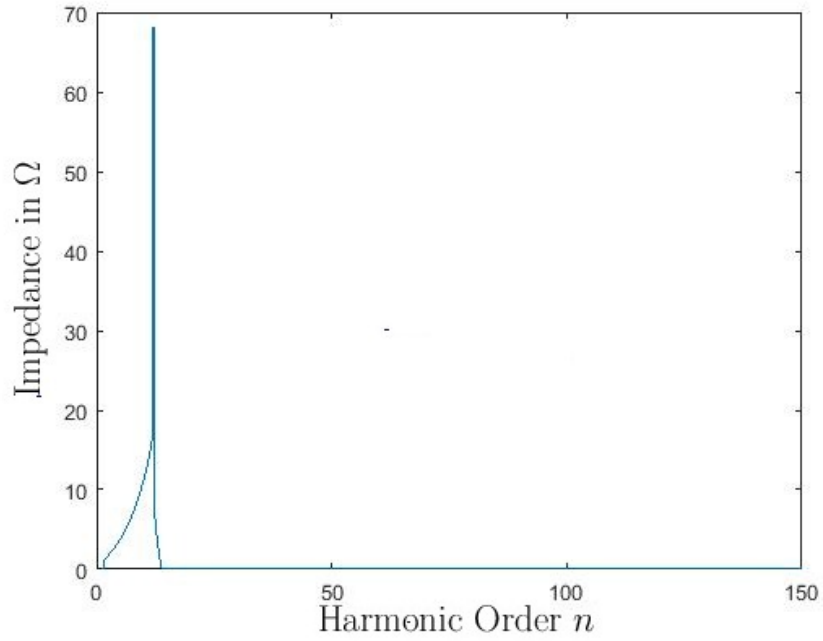

Figure 3.49: Mode-7 with Detuned Reactor and C Filter on Bus-5

Table 3.11: Comparison of Modal Analysis of Network with Detuned Reactor on 200 kVAr Capacitor and C Filter on Bus-5

	Mode Order without Detuned Reactor	Mode Order with Detuned Reactor and C Filter on Bus-5
Mode-1	125	68-70, 74-75
Mode-2	Multiple 69-70, 72-75, 88.5	
Mode-3	9.4, 47.9	75-80
Mode-4	76	9-15
Mode-5	32.5	70-72, 75-88
Mode-6	33, 41.5, 42.5, 111, 113, 117	9-12, 14
Mode-7	42, 113	12

The careful assessment of the result of comparison shows that the C-type filter results in to multiple peaks in different modes. However, only mode-3 shows the significant Modal impedance. It suppress the other modes, which observed in the results with only Detuned Reactor. If converter is having distributed harmonic spectrum, this may cause the trouble with operation of converter. So, to see the possible improvement, further analysis is carried out with High Frequency Filter, tuned above 11^{th} order. It is given in next section.

3.7.4 Modal Analysis with Detuned Reactor and High Frequency Filter on Bus-5

As an alternative high frequency tuned filter is installed at Bus-5. The result of Modal analysis of network with detuned reactor on 200 kVAr and 15 MVAr of high frequency filter on Bus-5 is compared with the Modal analysis of bare network i.e. without any compensation. The results are given in figure 3.51 to 3.57. Also the results are compared in table 3.13

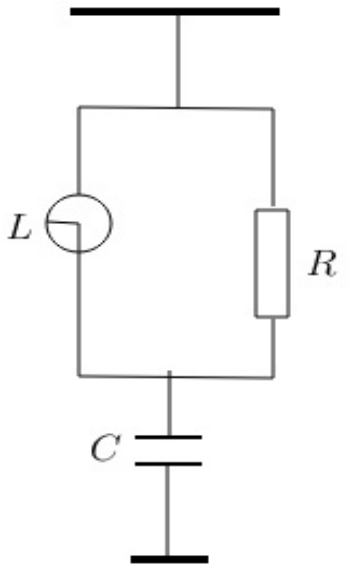

Figure 3.50: High Frequency Filter

Table 3.12: High Frequency Filter Parameters

High Frequency Filter	
C	$40\mu F$
f_h	$11^{th} Order$
L	$2.1mH$
R	50Ω

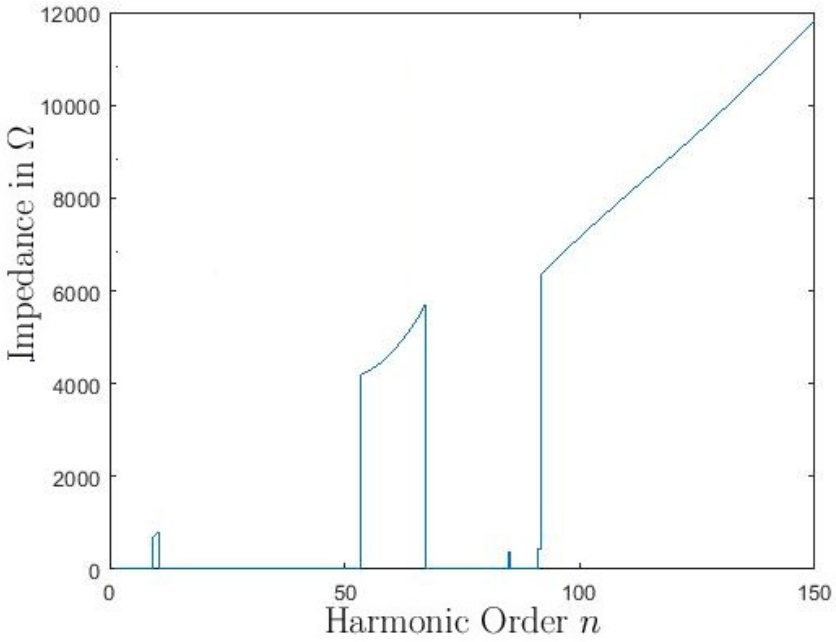

Figure 3.51: Mode-1 with Detuned Reactor and High Frequency Filter on Bus-5

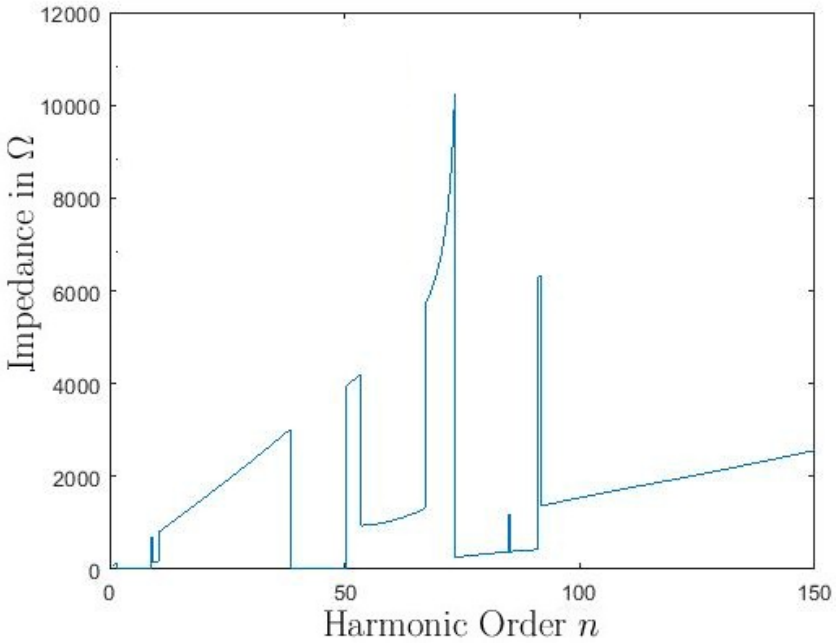

Figure 3.52: Mode-2 with Detuned Reactor and High Frequency Filter on Bus-5

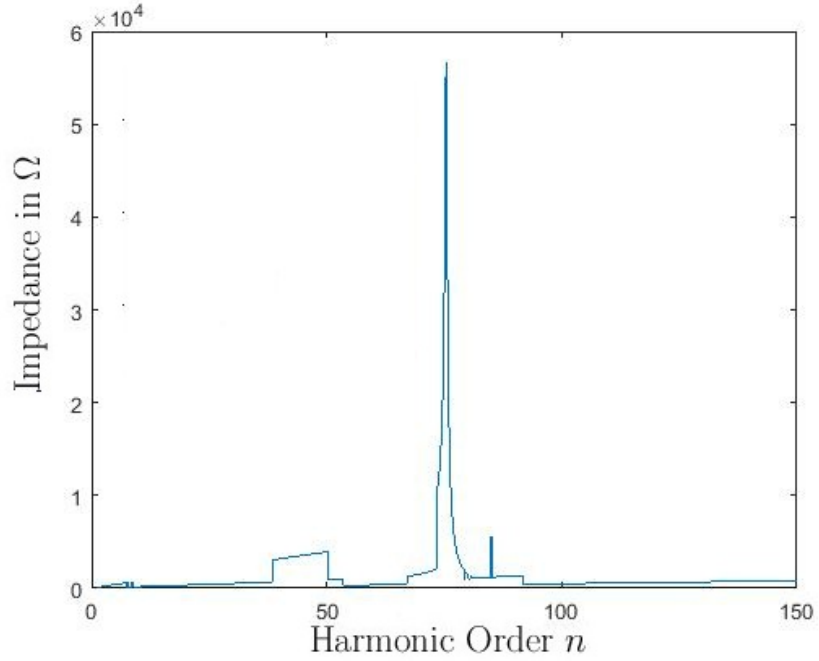

Figure 3.53: Mode-3 with Detuned Reactor and High Frequency Filter on Bus-5

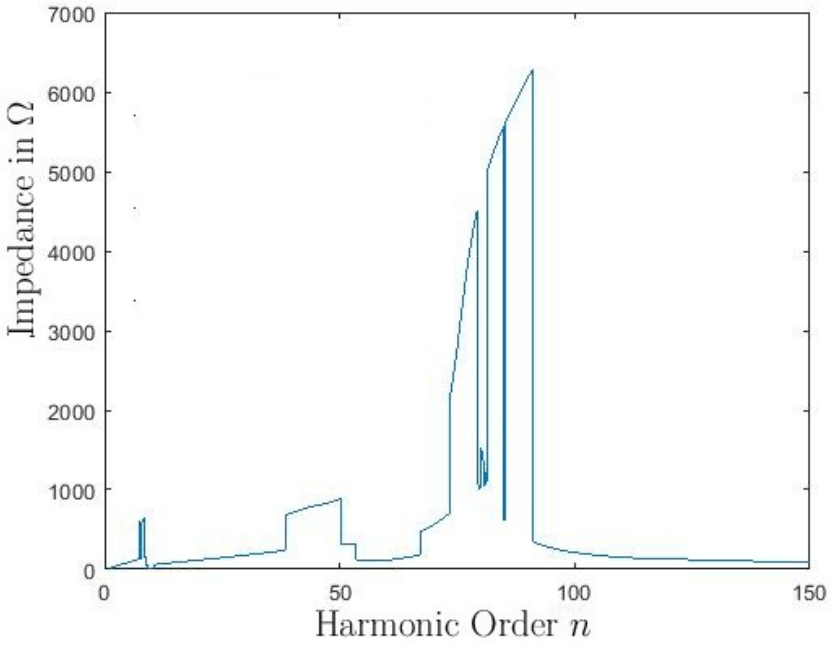

Figure 3.54: Mode-4 with Detuned Reactor and High Frequency Filter on Bus-5

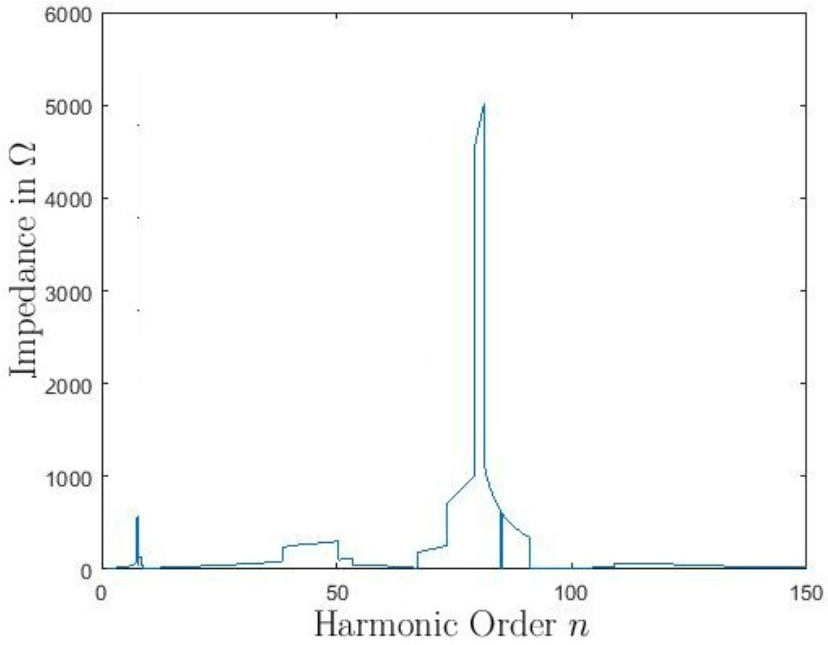

Figure 3.55: Mode-5 with Detuned Reactor and High Frequency Filter on Bus-5

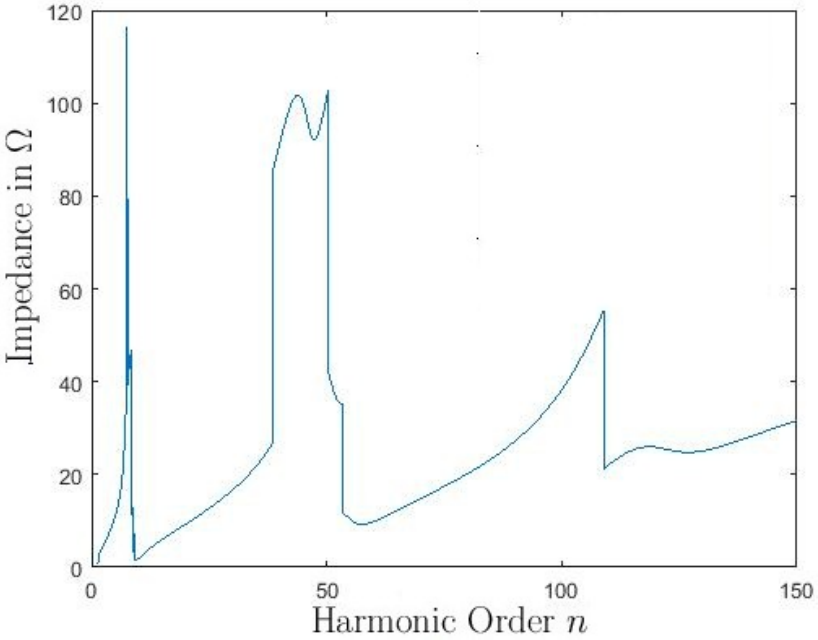

Figure 3.56: Mode-6 with Detuned Reactor and High Frequency Filter on Bus-5

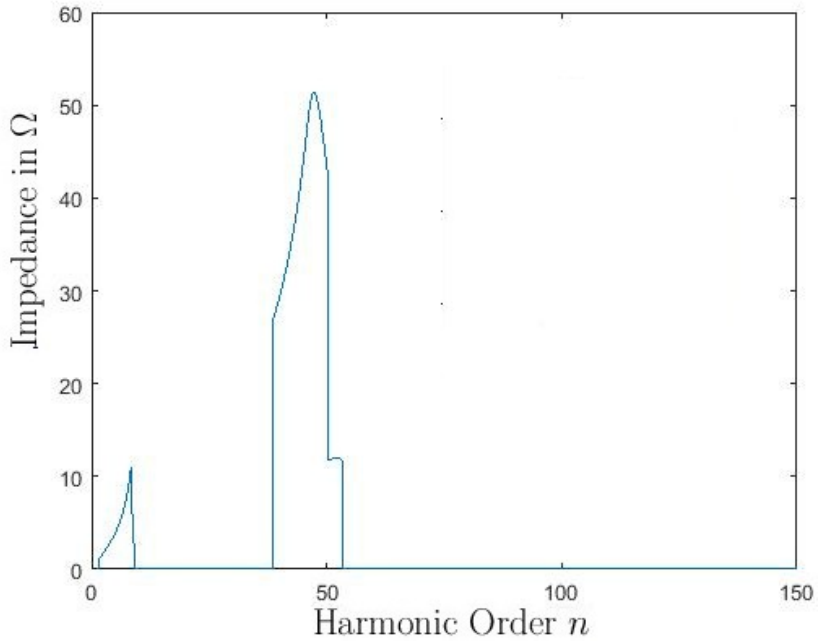

Figure 3.57: Mode-7 with Detuned Reactor and High Frequency Filter on Bus-5

Table 3.13: Comparison of Modal Analysis Network and Network with Detuned Reactor on 200 kVAr Capacitor and High Frequency Filter on Bus-5

	Mode Order without Detuned Reactor	Mode Order with Detuned Reactor and High Frequency Filter on Bus-5
Mode-1	125	53 - 67
Mode-2	Multiple (< 50)	62 - 73, 91
Mode-3	9.4, 47.9	75.6 (Significant)
Mode-4	76	multiple & unclear
Mode-5	32.5	80
Mode-6	33, 41.5, 42.5, 111, 113, 117	Not Significant
Mode-7	42, 113	Not Significant

Table 3.14: Order of Critical Frequencies at Various Buses

	Bus1	Bus 2	Bus 3	Bus 4	Bus 5	Bus 6	Bus 7
f_{h1}	9.4	125	76	32.5	117	33.3	
f_{h2}		50 - 150	32.5	65 -120	33.3		
f_{h3}		102 - 118	33.3	33.3	65 -120		
f_{h4}		110	113				
f_{h5}		41.8	65-120				
f_{h6}		113.3					

The comparative analysis of different modes with bare network (without any filter) and modes with High Frequency Damped Filter (11^{th} order) is given in table (3.13). From the result analysis it is clear that the High Frequency Filter is effective in reduction of Modal impedances as compared to C-type Filter. Only one critical mode is observed (Mode-3). The Critical Frequency observed is of 75.6^{th} order (Mode-3). Otherwise, all other Modal impedances are inductive in nature and no apparent resonance is observed. Only Mode-3 is critical and it should be addressed. The participation factor shows that

the sensitivity of Mode-3 with respect to for buses 1 to 7 are 0.1846, 0.2517, 0.2876, 0.2797, 0, 0 and 0 respectively. This seems to be quite distributed mode and can be controlled from this buses only. The High Frequency Filter is connected on Bus-5 and this bus has zero participation factor, so we may say that the High Frequency Filter has not been directly affecting Mode-3. This is actually a Mode-4 of the bare network.

3.7.5 Optimization of Harmonic Filter

The different type of filter affects modes differently. To achieve overall good results, an attempt it made to optimize the filter parameter. Also, its effectiveness is checked with respect to the different bus locations. Four different type of filters as shown in figure (3.58) are considered. At a time, first the bus loacation is fixed and then filter parameters for each filter type are optimized using Simulated Annealing technique with objective function as already defined. The results are given here in graphical form in figure (3.59) to (3.68) and also given tabular form in table (3.15).

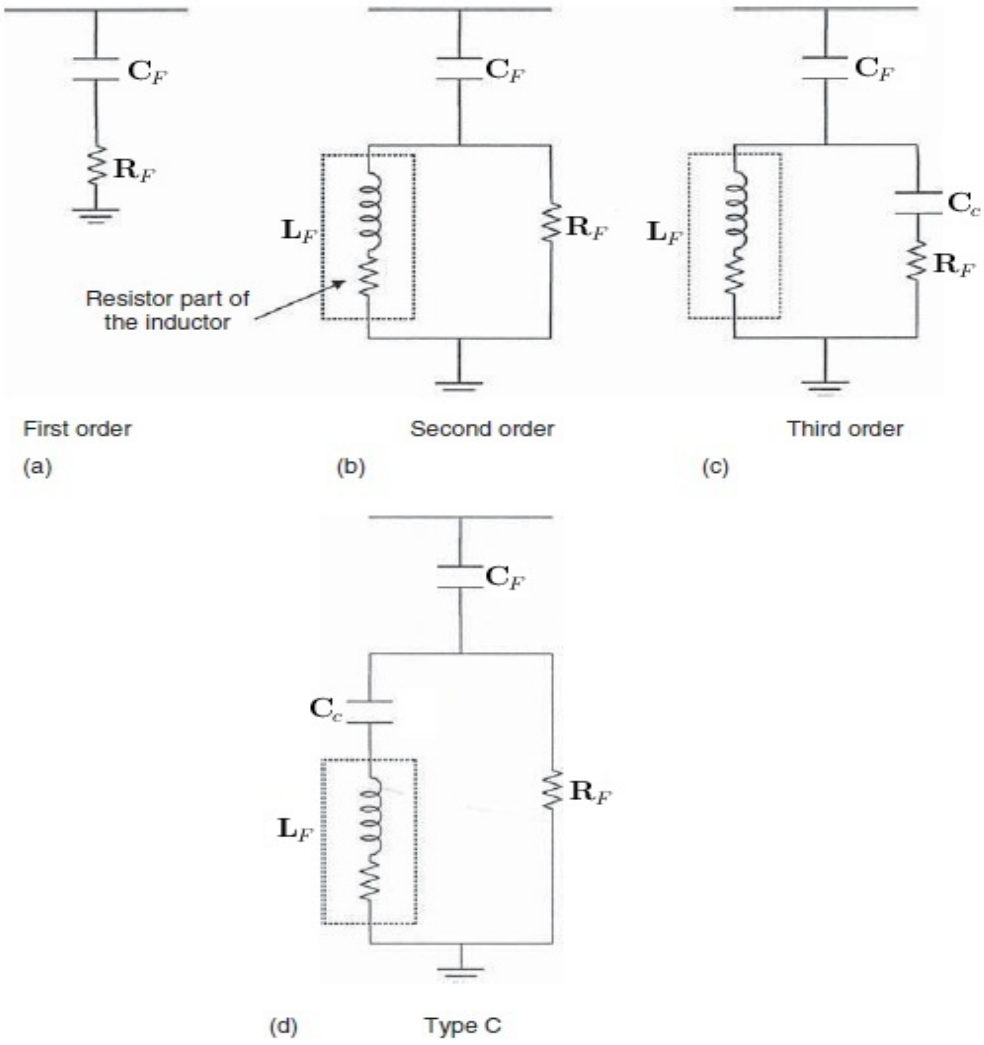

Figure 3.58: Different Types of Filter

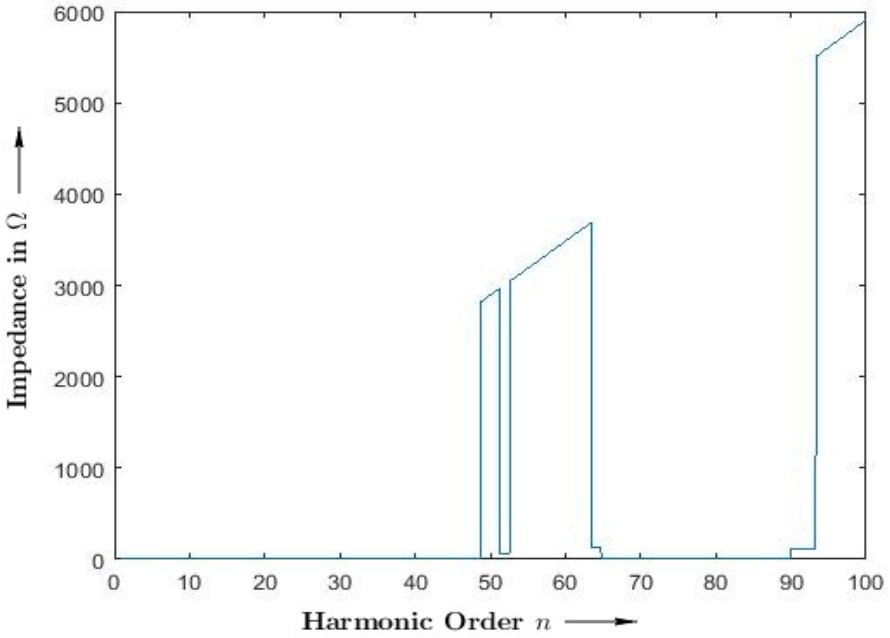

Figure 3.59: Mode-1 with Optimized First Order Filter on Bus-3

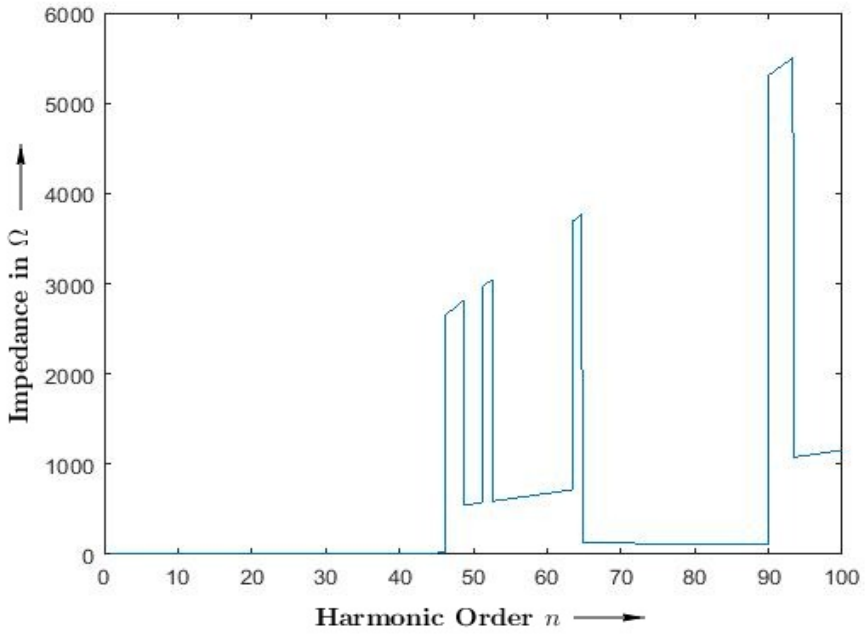

Figure 3.60: Mode-2 with Optimized First Order Filter on Bus-3

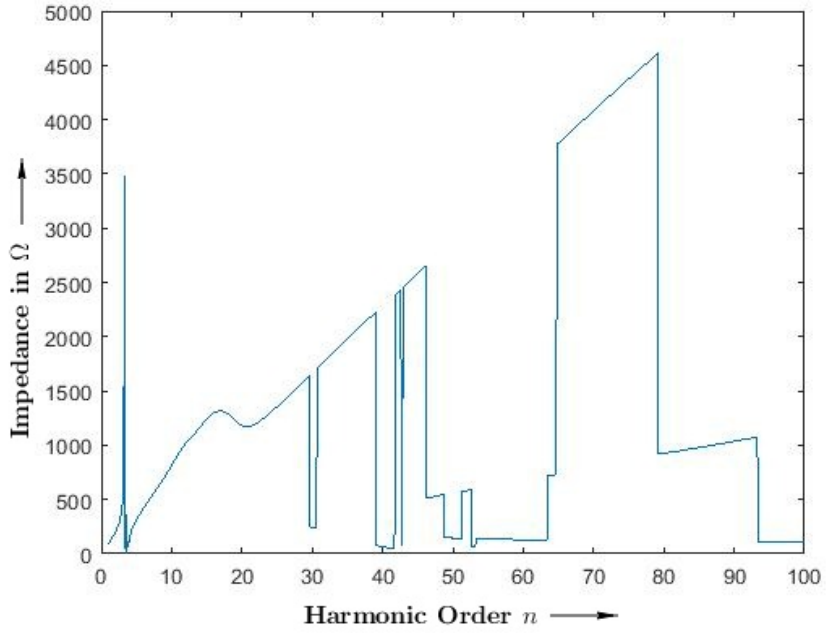

Figure 3.61: Mode-3 with Optimized First Order Filter on Bus-3

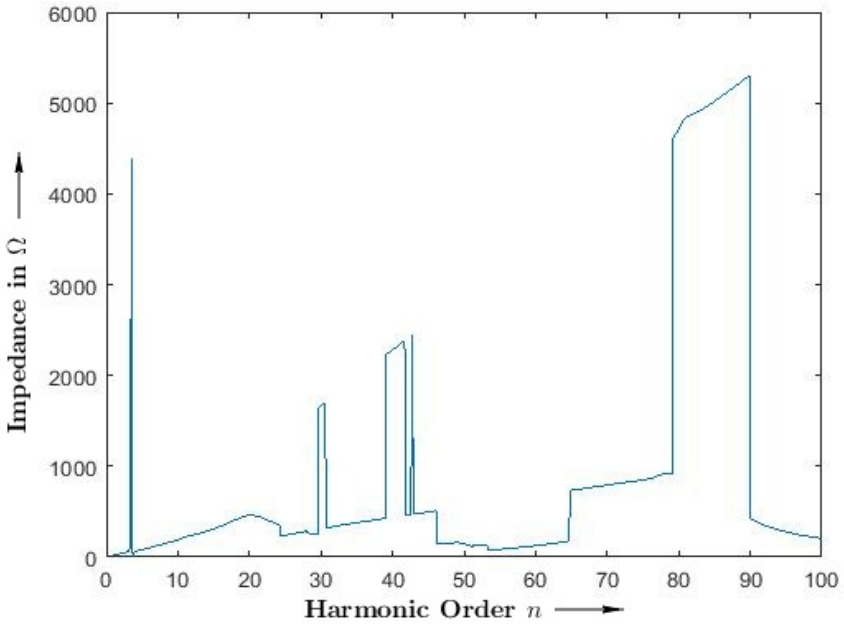

Figure 3.62: Mode-4 with Optimized First Order Filter on Bus-3

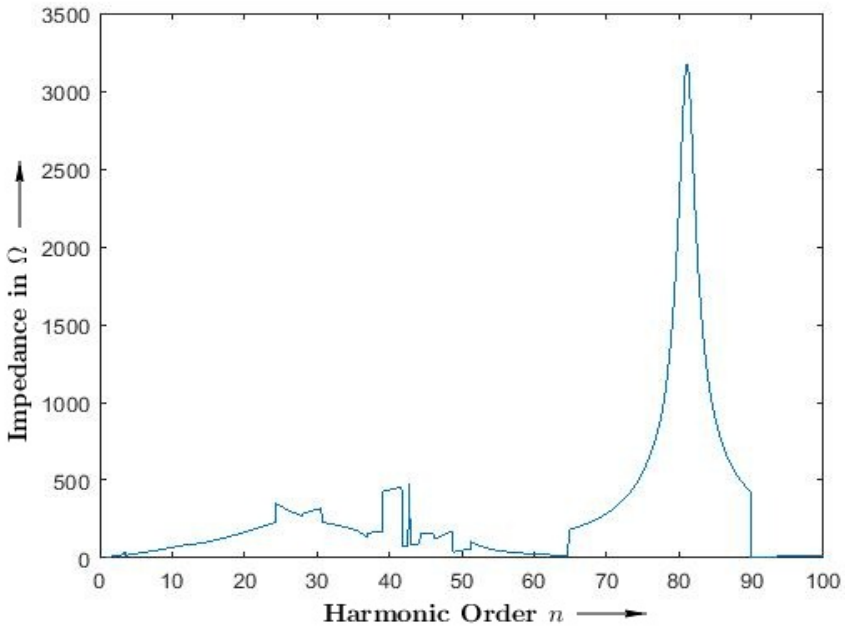

Figure 3.63: Mode-5 with Optimized First Order Filter on Bus-3

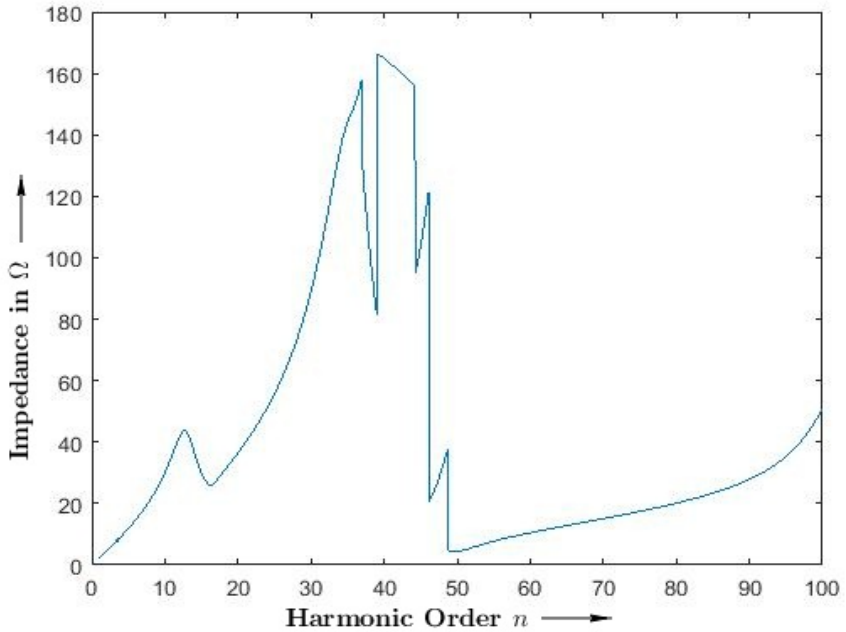

Figure 3.64: Mode-6 with Optimized First Order Filter on Bus-3

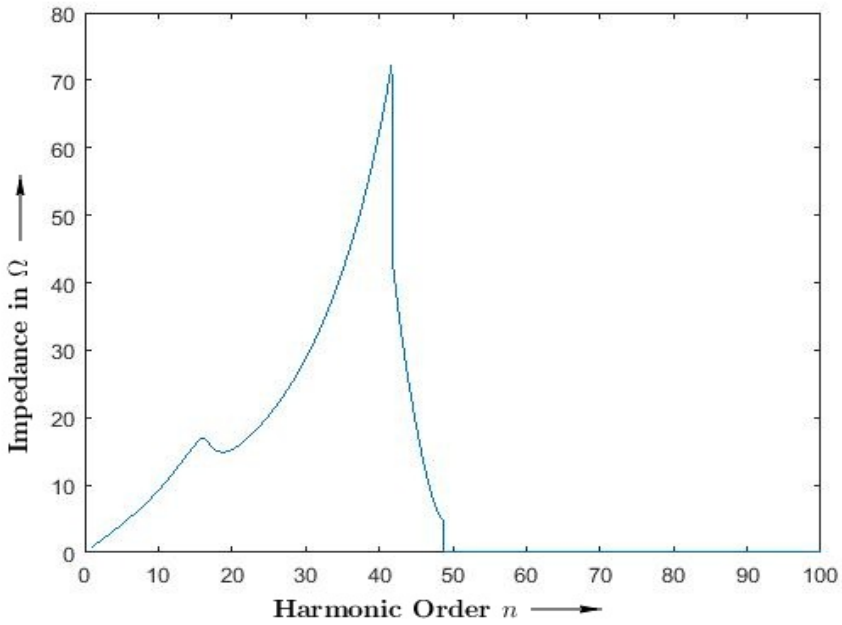

Figure 3.65: Mode-7 with Optimized First Order Filter on Bus-3

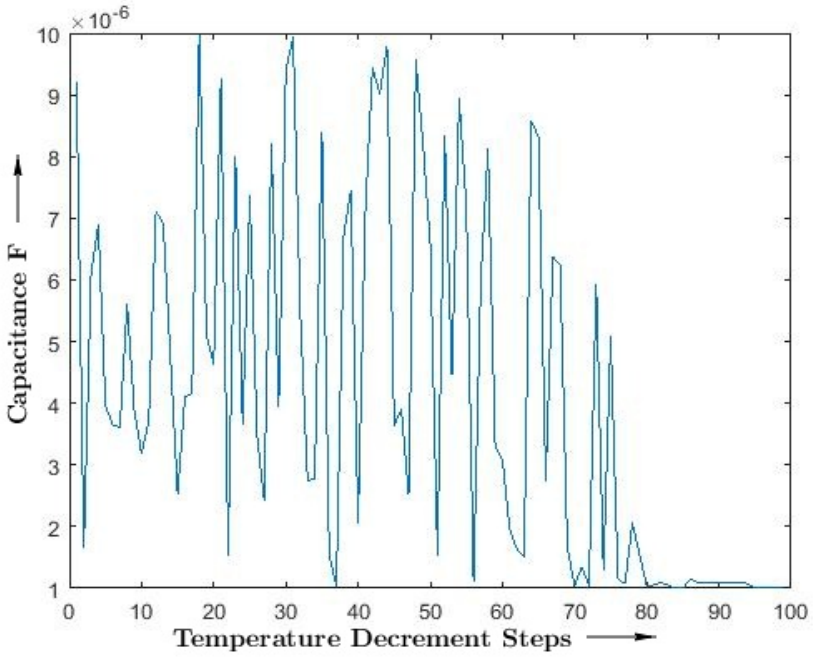

Figure 3.66: Capacitance of Optimized First Order Filter on Bus-3

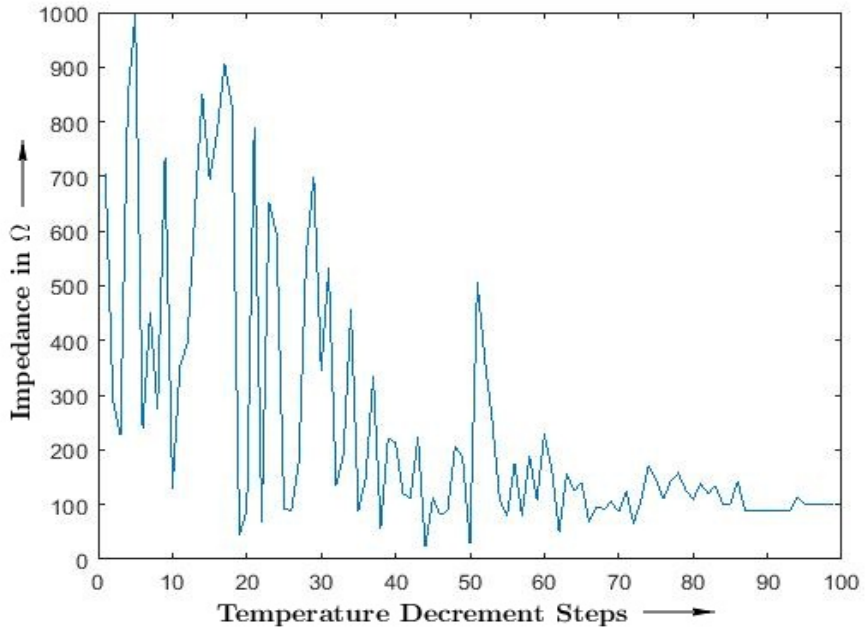

Figure 3.67: Resistance of Optimized First Order Filter on Bus-3

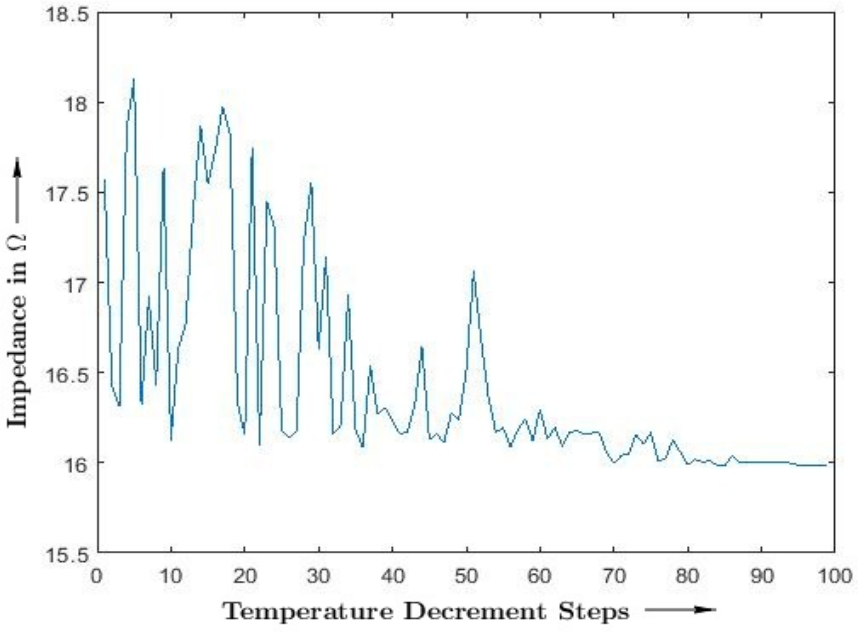

Figure 3.68: Impedance of Optimized First Order Filter on Bus-3

Table 3.15: Optimization of Different Filter Types

Sr. No	Bus No	Filter Type	Filter Parameter	Impedance Value	Comment
1	Bus-3	First Order	$C_F = 1.016\ \mu F$ $R_F = 100.57\ \Omega$	$Z_F = 15.98\ \Omega$	Best Filter-Location
2	Bus-3	Second Order	$C_F = 1.365\ \mu F$ $R_F = 79.77\ \Omega$ $L_F = 15mH$	$Z_F = 16.66\ \Omega$	
3	Bus-3	Third Order	$C_F = 8.976\ \mu F$ $C_c = 16.48\ nF$ $R_F = 24.98\ \Omega$ $L_F = 1.3\ mH$	$Z_F = 18.36\ \Omega$	
4	Bus-3	C-Type	$C_F = 2.304\ \mu F$ $C_c = 1.2\ mF$ $R_F = 101.58\ \Omega$ $L_F = 8.7\ mH$	$Z_F = 16.36\ \Omega$	
5	Bus-4	First Order	$C_F = 1.028\ \mu F$ $R_F = 14.51\ \Omega$	$Z_F = 19.42\ \Omega$	
6	Bus-4	Second Order	$C_F = 1.046\ \mu F$ $R_F = 19.14\ \Omega$ $L_F = 12mH$	$Z_F = 19.43\ \Omega$	
7	Bus-4	Third Order	$C_F = 4.79\ \mu F$ $C_c = 17.59\ nF$ $R_F = 617.39\ \Omega$ $L_F = 1.0\ mH$	$Z_F = 19.85\ \Omega$	
8	Bus-4	C-Type	$C_F = 1.041\ \mu F$ $C_c = 2.6\ mF$ $R_F = 22.9\ \Omega$ $L_F = 3.8\ mH$	$Z_F = 19.44\ \Omega$	

Contd. ...

Table 3.15 (Contd.) ...

Sr. No	Bus No	Filter Type	Filter Parameter	Impedance Value	Comment
9	Bus-5	First Order	$C_F = 30.34\ \mu F$ $R_F = 50.13\ \Omega$	$Z_F = 29.033\ \Omega$	
10	Bus-5	Second Order	$C_F = 35.79\ \mu F$ $R_F = 92.56\ \Omega$ $L_F = 1.2mH$	$Z_F = 33.11\ \Omega$	
11	Bus-5	Third Order	$C_F = 31.79\ \mu F$ $C_c = 1.863\ nF$ $R_F = 940.45\ \Omega$ $L_F = 1.1\ mH$	$Z_F = 33.40\ \Omega$	
12	Bus-5	C-Type	$C_F = 36.13\ \mu F$ $C_c = 9.1\ mF$ $R_F = 145.28\ \Omega$ $L_F = 1.1\ mH$	$Z_F = 33.11\ \Omega$	

The result tabulated here suggests the good location and type of filter to be used to achieve the overall good results. According to this results, the 1^{st} order filter at Bus-3 is best solution. It shall be further evaluated to check the violation of harmonic voltage with harmonic current spectrum of different converter of different make. It is given in the next section.

3.7.5.1 Effect of Optimized First Order Filter on Network Impedance

Effect of inclusion of optimized filter of first order can seen in following figures. The impedance of network without filter and network with filter are compared here. The impedance is basically the impedance voltage in response to the unit harmonic current injection at Bus-1. It is derived by either inverting the admittance matrix or by using relation between nodal impedance and Modal impedance as given in Modal Analysis section.

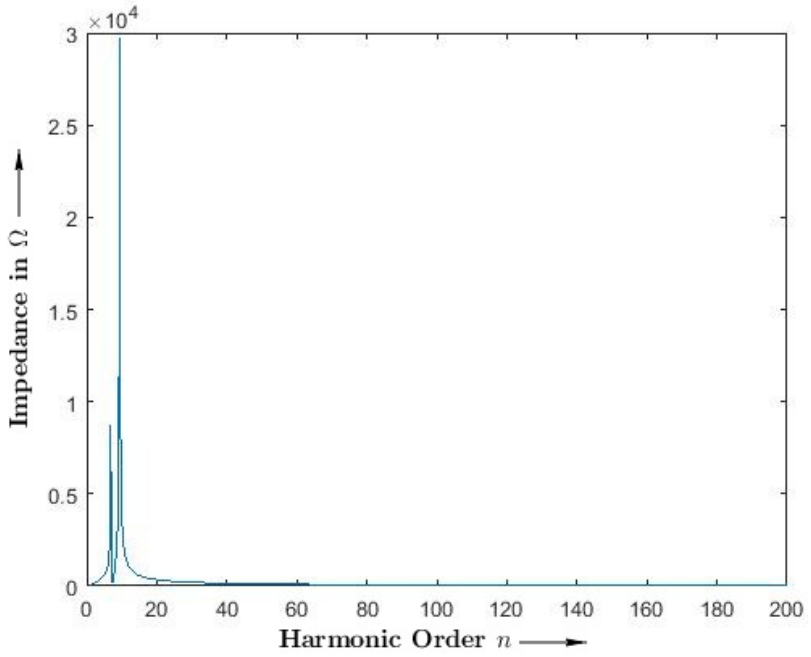

Figure 3.69: Impedance at Bus-1 without Optimized First Order Filter

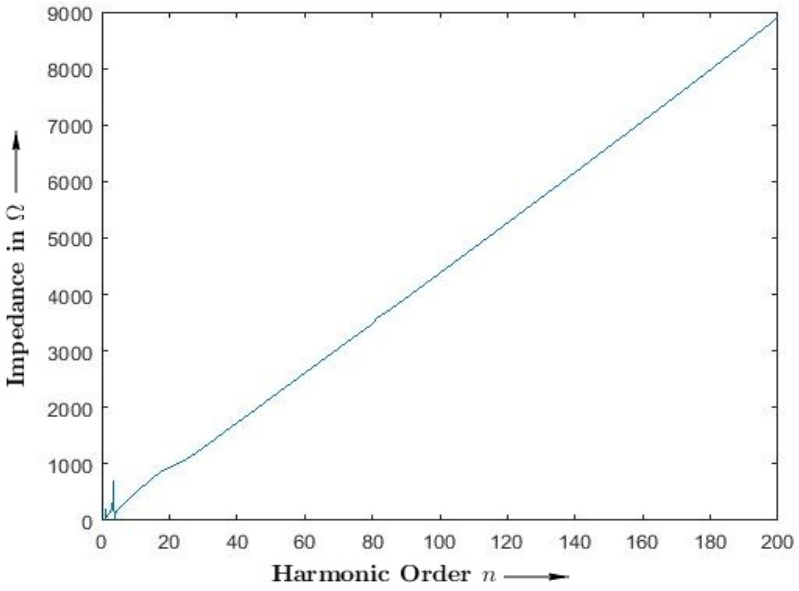

Figure 3.70: Impedance at Bus-1 with Optimized First Order Filter

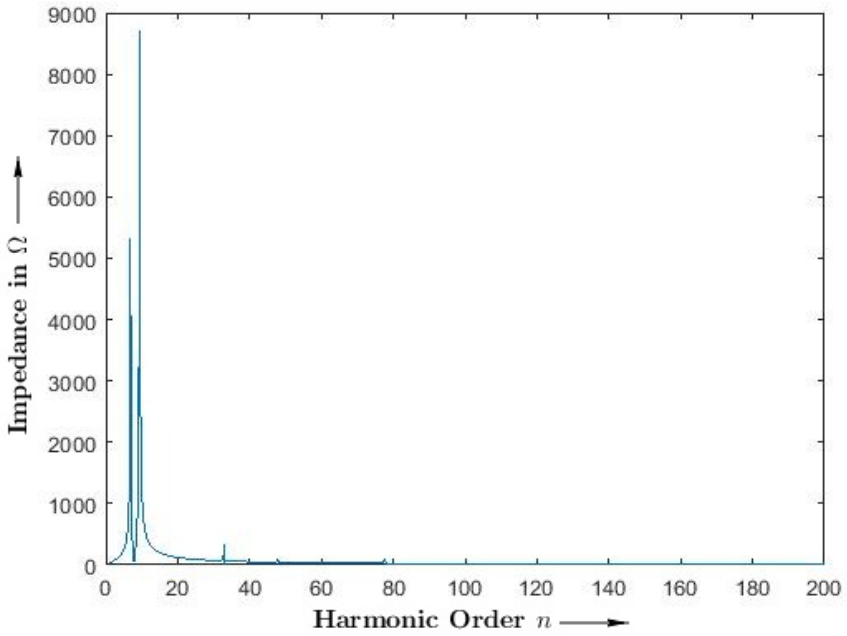

Figure 3.71: Impedance at Bus-2 without Optimized First Order Filter

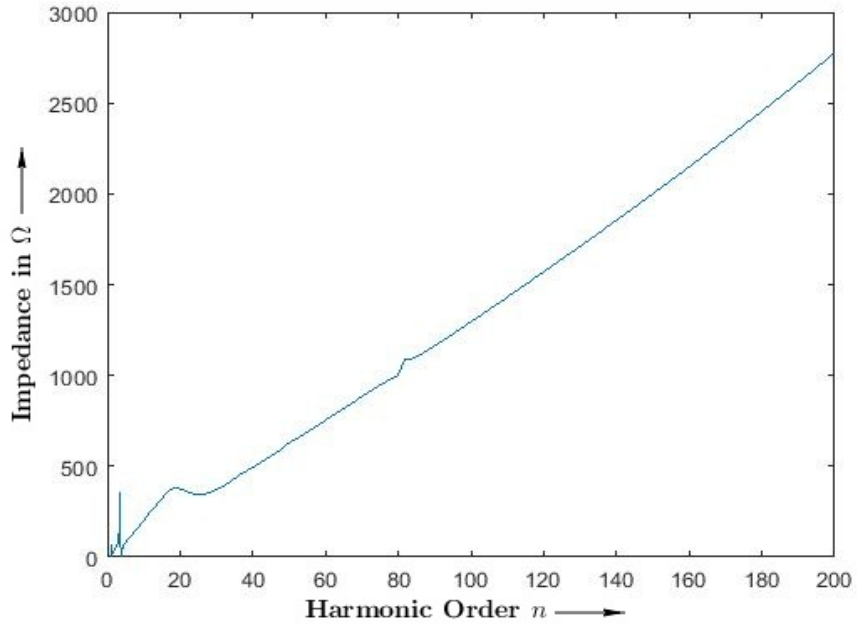

Figure 3.72: Impedance at Bus-2 with Optimized First Order Filter

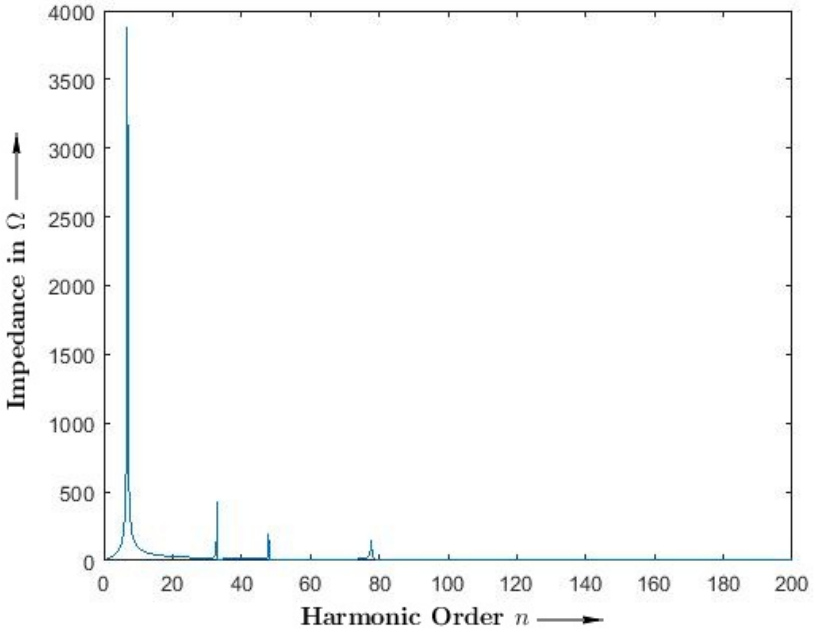

Figure 3.73: Impedance at Bus-3 without Optimized First Order Filter

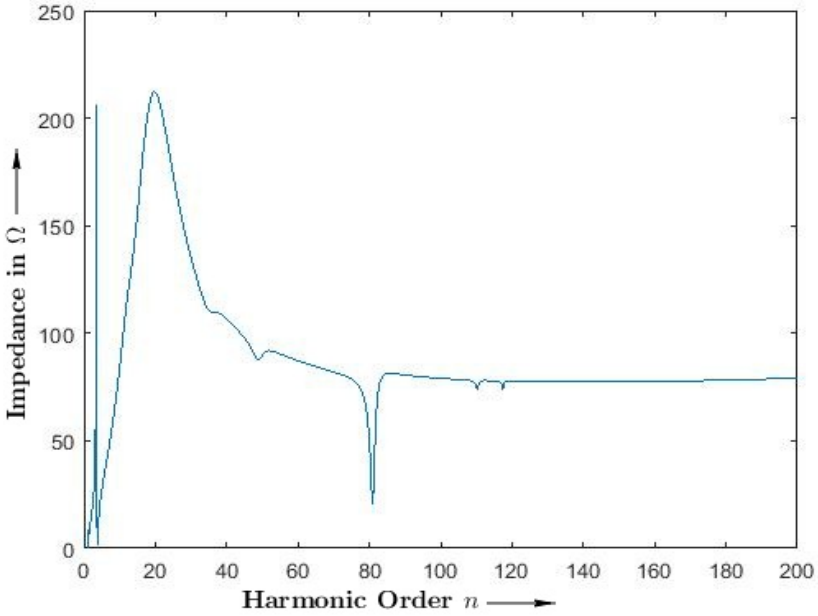

Figure 3.74: Impedance at Bus-3 with Optimized First Order Filter

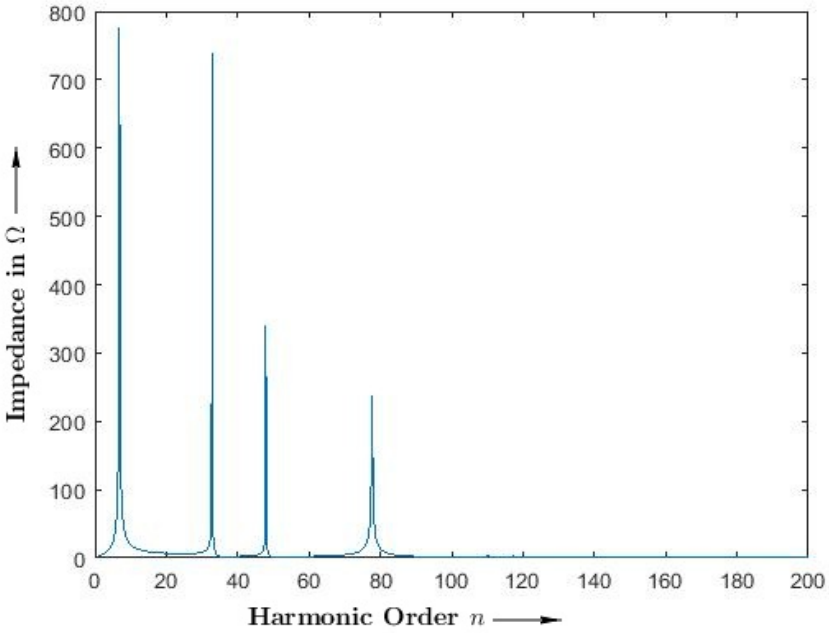

Figure 3.75: Impedance at Bus-4 without Optimized First Order Filter

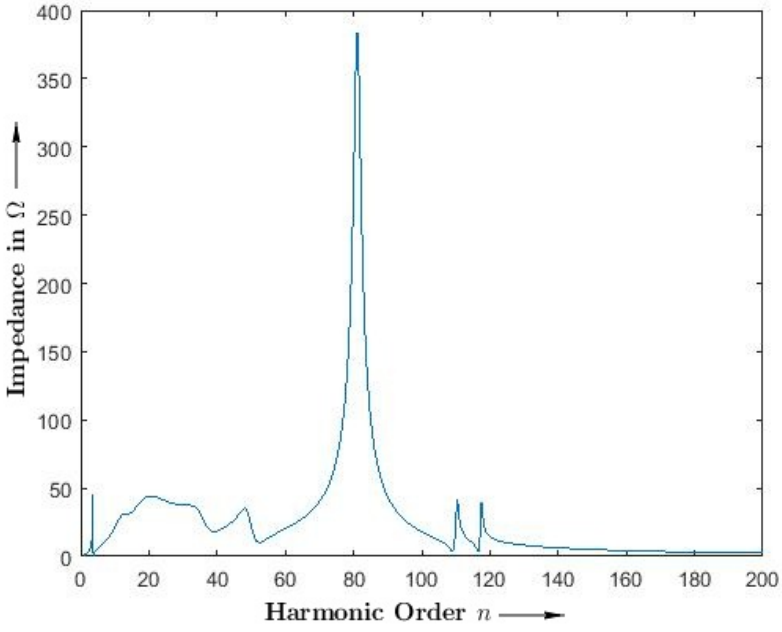

Figure 3.76: Impedance at Bus-4 with Optimized First Order Filter

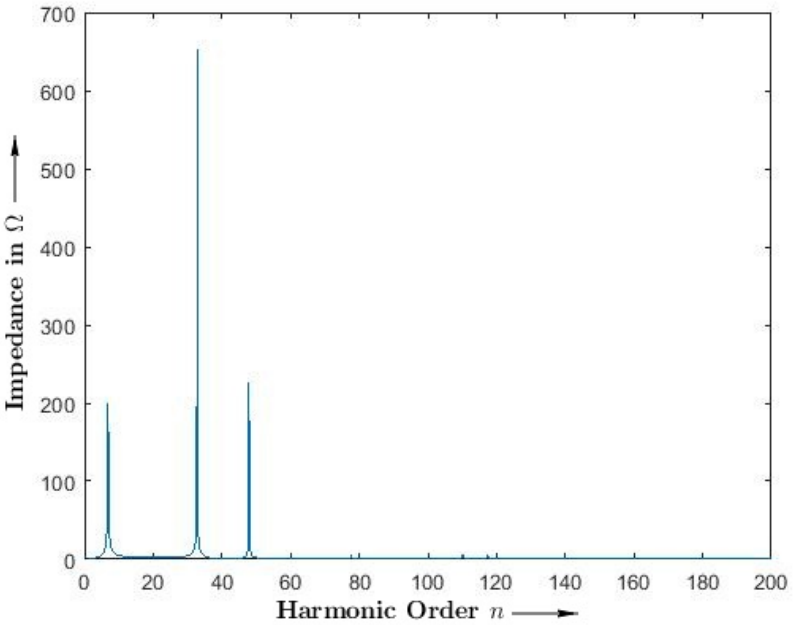

Figure 3.77: Impedance at Bus-5 without Optimized First Order Filter

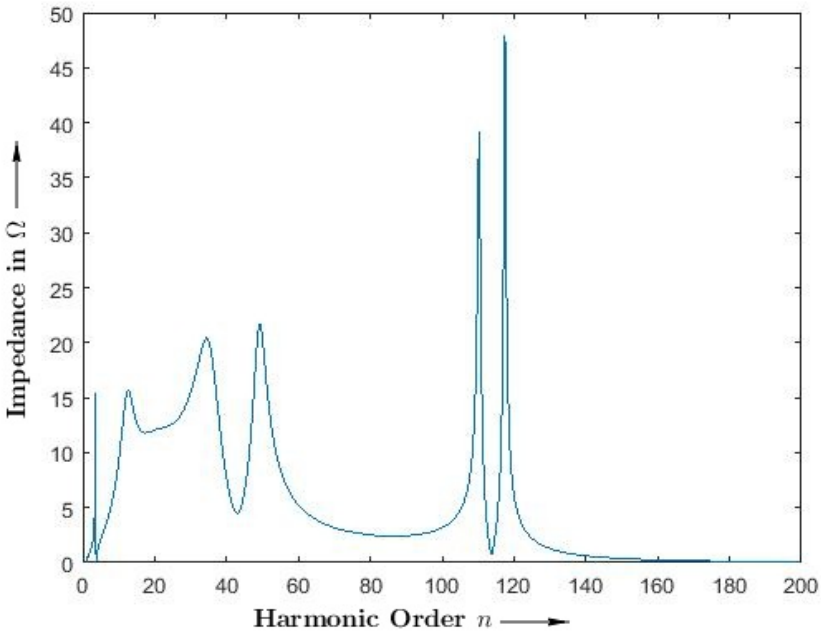

Figure 3.78: Impedance at Bus-5 with Optimized First Order Filter

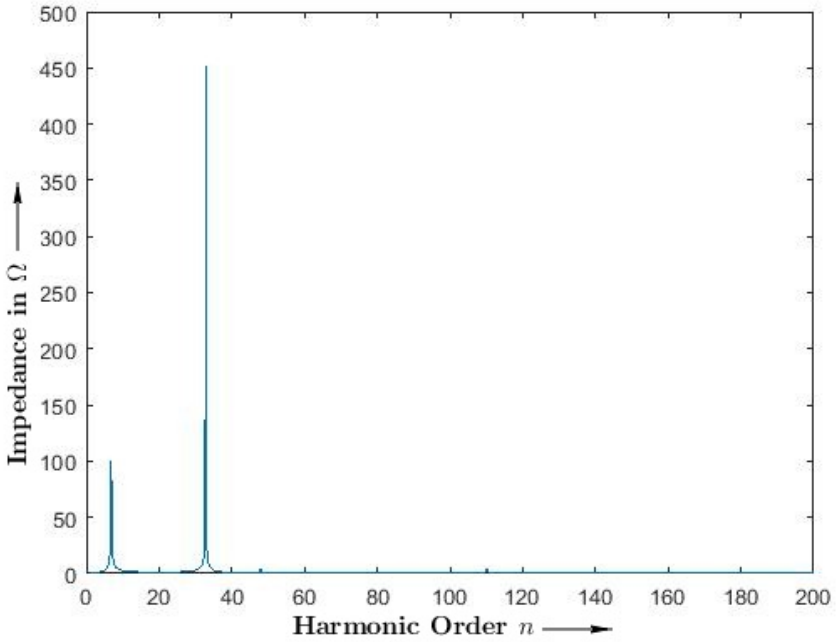

Figure 3.79: Impedance at Bus-6 without Optimized First Order Filter

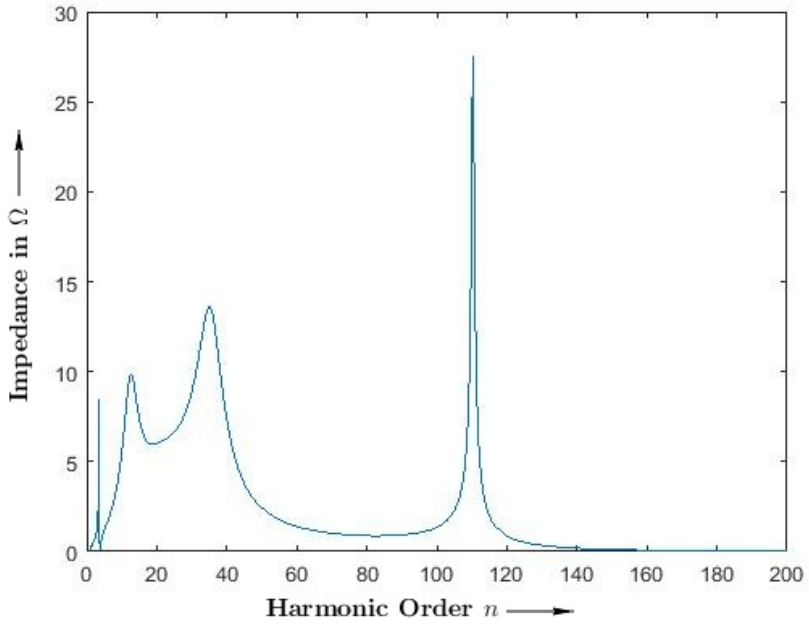

Figure 3.80: Impedance at Bus-6 with Optimized First Order Filter

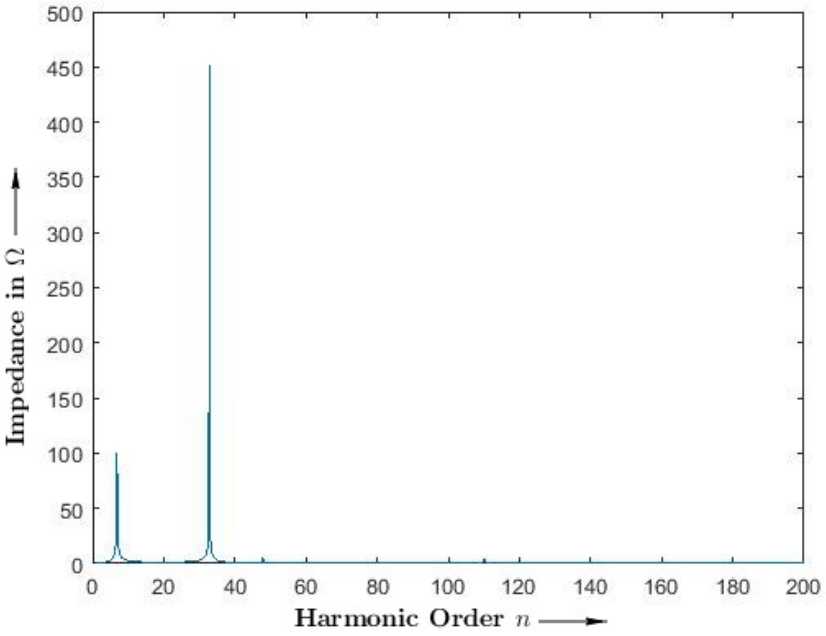

Figure 3.81: Impedance at Bus-7 without Optimized First Order Filter

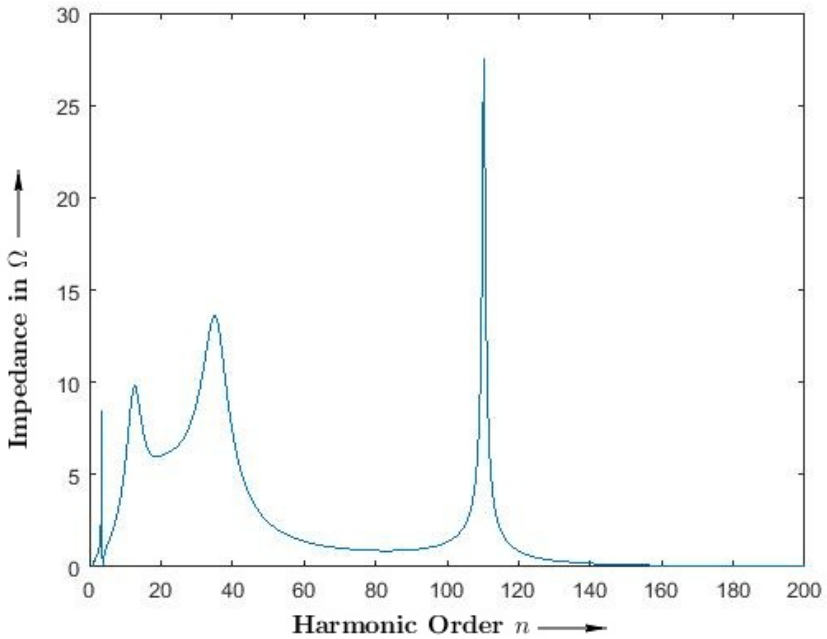

Figure 3.82: Impedance at Bus-7 with Optimized First Order Filter

The result shows that there is overall reduction in nodal impedances (Bus impedances). This proves the effectiveness the first order filter. But, it is yet to be checked for IEEE

compliance. It is given here.

3.7.5.2 Compliance to IEEE 519 - 1992/2014 Standard

To verify whether requirements of power quality standard is complied with or not, the actual harmonic current spectrum of two different converters are taken from [335] to check the harmonic voltage distortion at different buses. The one wind turbine is of Aban Kenetech (Type-I) and second is of unknown make (Type-II). The Type - I turbine is operated at around 5 kHz switching frequency, whereas Type-II turbine is operated at 20 kHz frequency. The waveforms has been captured with 25 kHz sampling rate. The harmonic spectrum of Type-I Wind Turbine exhibits two peak around 85^{th} and 170^{th} order. It is likely to originating from switching frequency around 4.3 kHz. The two current specturms are given here in figure (3.83) and (3.84).

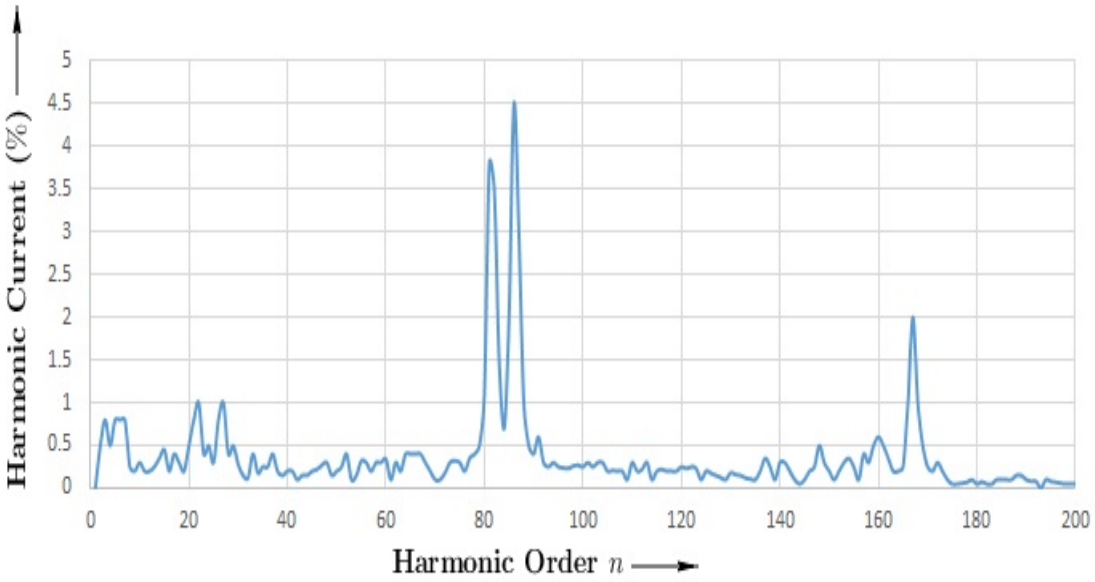

Figure 3.83: Harmonic Current Spectrum of Wind Turbineof Type-I

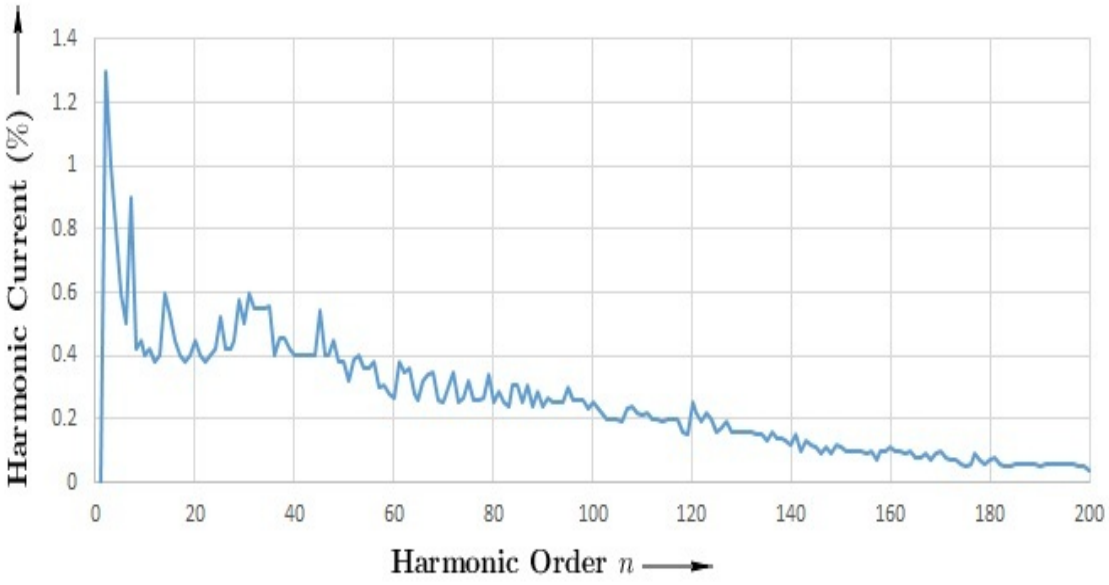

Figure 3.84: Harmonic Current Spectrum of Wind Turbineof Type-II

The harmonic current is injected at Bus-1 and resulting harmonic voltage are calculated. The results are given here in figure (3.85) to (3.88).

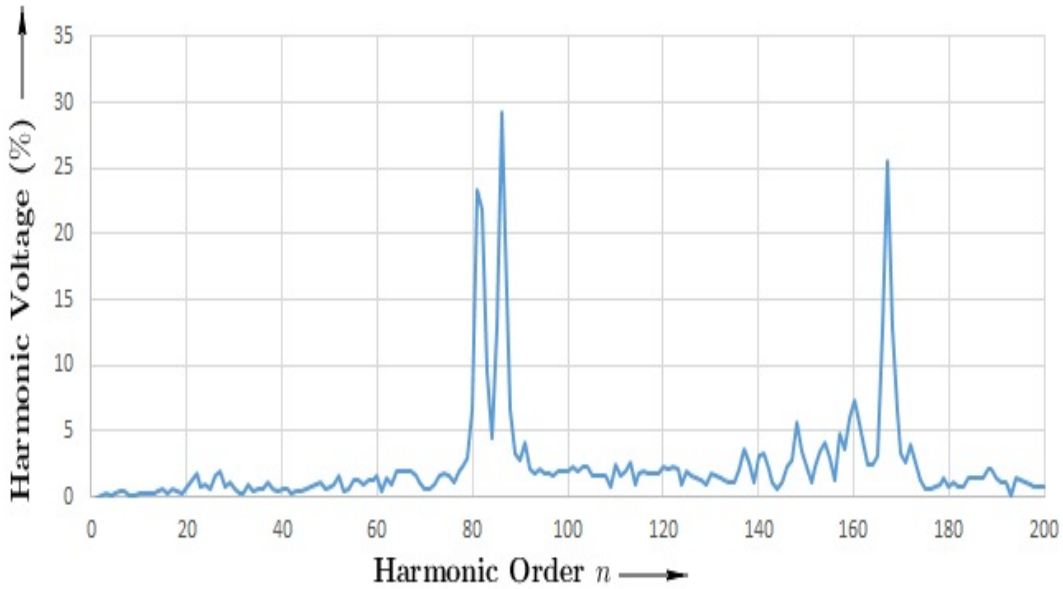

Figure 3.85: Harmonic Voltage at Bus-1 with Wind Turbine of Type-I

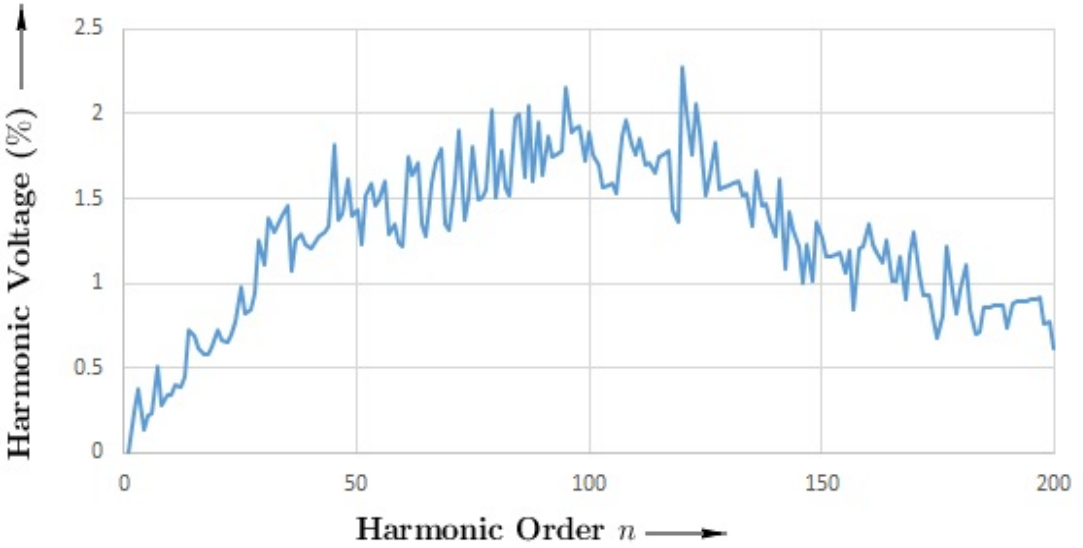

Figure 3.86: Harmonic Voltage at Bus-1 with Wind Turbine of Type-II

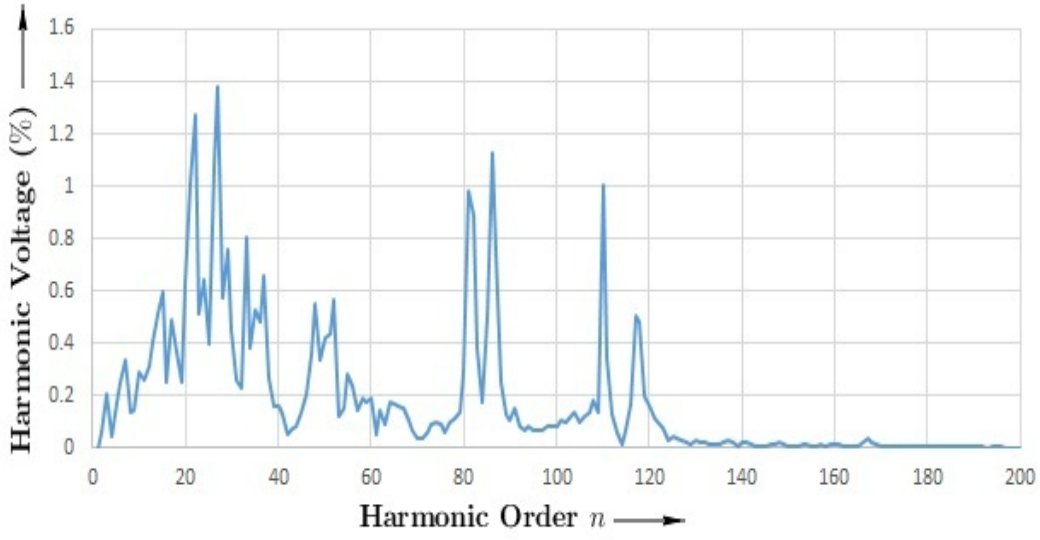

Figure 3.87: Harmonic Voltage at Bus-5 with Wind Turbine of Type-I

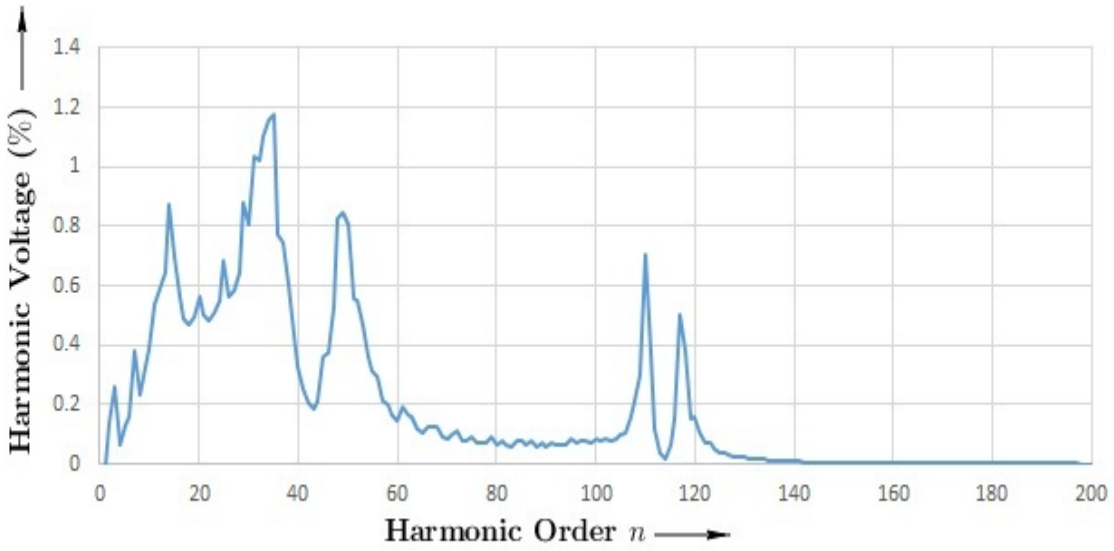

Figure 3.88: Harmonic Voltage at Bus-5 with Wind Turbine of Type-II

From above results, it is clear that the harmonic voltage at Point of Common Coupling (PCC) is under limit for both the converters. However, Type-I converter produces large harmonic voltage at Wind Turbine Bus. This may hamper the operation of converters. Several such incidents have been reported from the field where the converter trips under the overvoltage. So, this type of prior study helps in planning and successful integration of WTG into existing power system. The Type-II converter produces lower harmonics but it causes higher losses in converter due to high switching frequency. So, there is a tradeoff between the harmonic level and power losses. It suggests that the switching frequency has to be decided carefully. In short, here the Type- II successfully meets the IEEE 519-1992/2014 standard requirement, even under the full load condition and is more suitable for network under study.

3.8 Conclusion

Harmonic stability is an important aspects of renewable generation power technologies. The harmonic generation not only occurs losses in the network but also affects the operation of power electronic based converters negatively and inhibits the full scale operation of Wind Turbines. Also, the resulting voltage distrotion in the network may affect the other consumers connected in the network. The Modal analysis is an effective and easy

to use tool to analyse the network for any possible problems due to harmonic resonance. Using Modal analysis, the harmonic filter can also be optimized and is first time demonstrated in this work. By exploiting the sensitivity analysis of modes, the root cause of harmonic resonance can be pointed out and thus can be dealt with effectively. The key advantage of Modal analysis is the easy formulation, where other methods are lacking. The substantial take away from this work is that, the network configuration and converter type needs to be examined prior to connection of WTG. Also, for some converters, the network conditioning/modification is required prior to connecting the particular type of WTG to the network. Also, the switching frequency plays an important role in capacity utilization of WTG.